AD-A124 778   DYNAMIC CHARACTERISTICS OF AERIAL REFUELING SYSTEMS(U)   1/1
              AIR FORCE INST OF TECH WRIGHT-PATTERSON AFB OH SCHOOL
              OF ENGINEERING   T J CARTER DEC 82 AFIT/GAE/AA/82D-4
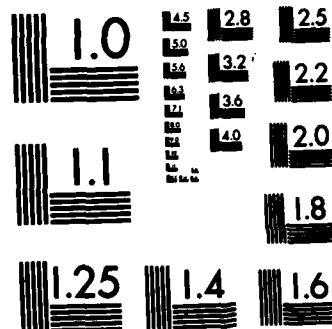
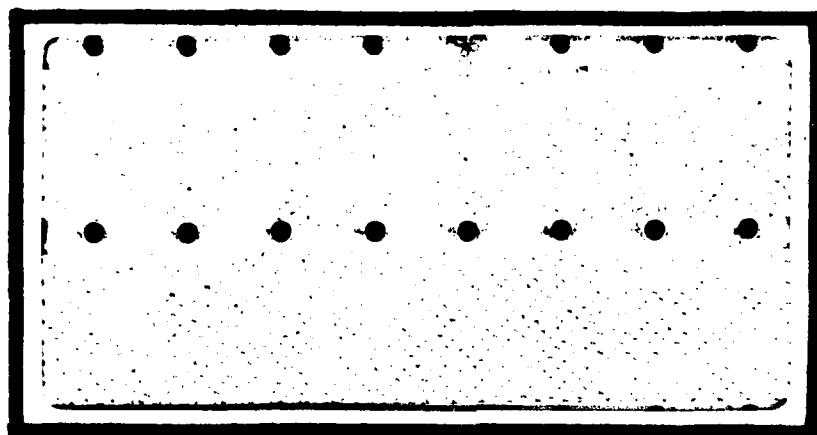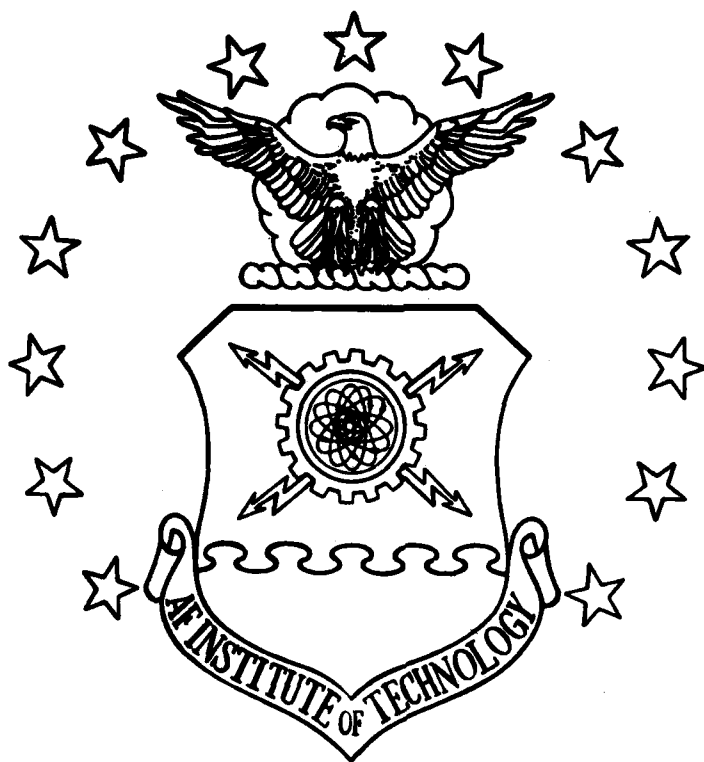UNCLASSIFIED   .F/G 1/2   NL

END
FILMED
I N
DTIC

MICROCOPY RESOLUTION TEST CHART
NATIONAL BUREAU OF STANDARDS-1963-A

AF INSTITUTE OF TECHNOLOGY

DEPARTMENT OF THE AIR FORCE
AIR UNIVERSITY (ATC)

AIR FORCE INSTITUTE OF TECHNOLOGY

Wright-Patterson Air Force Base, Ohio

83   02   022120

DYNAMIC CHARACTERISTICS OF
AERIAL REFUELING SYSTEMS

THESIS

AFIT/GAE/AA/82D-4   Thomas J.Carter III
                      Capt   USAF

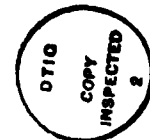Approved for public release; distribution unlimited.

DYNAMIC CHARACTERISTICS OF

AERIAL REFUELING SYSTEMS

THESIS

Presented to the Faculty of the School of Engineering

of the Air Force Institute of Technology

Air University

In Partial Fulfillment of the

Requirements for the Degree of

Master of Science

by

Thomas J. Carter III, BME

Captain   USAF

Graduate Aeronautical Engineering

December 1982

Accession For		
NTIS GRA&I		☒
DTIC TAB		☐
Unannounced		☐
Justification		
By		
Distribution/		
Availability Codes		
	Avail and/or	
Dist	Special	
A		

ACKNOWLEDGMENTS

ii

Contents

List of Figures

List of Tables

List of Symbols

A	Area	in^2
A_v	Effective Valve Area	in^2
A_{vo}	Full Flow Valve Area	in^2
c	Sonic Velocity	in/sec
C_d	Discharge Coefficient	
K	Valve Position	% Open
L	Length	in
$L(\ )$	Line Number $(\ )$	
$\dot{m}$	Mass Rate of Flow	in^3/sec
P	Pressure	lb_f/in^2
Q	Flowrate	in^3/sec
T	Time	sec
t	Time	sec
T_c	Valve Closure Time	sec
V	Velocity	in/sec
$\int$	Density	$(lb_f\text{-}sec^2)/in^4$

Abstract

Two aircraft refueling system configurations were simulated
using HYTRAN, an existing transient flow analysis computer program.
Transient pressure response subsequent to downstream valve closure
was investigated for the KC-135 and a laboratory test rig and
compared to available experimental data and previous research.
Parametric studies were performed of system variables: valve closure
time, valve area versus time (closure curves), and variations in
surge attenuation components (surge boot, accumulators). A typical
closure curve for quick disconnects was approximated and verified.
The simulation results compared favorably with experimental data
and previous work. Transient pressure was found to be sensitive to
accumulator or surge boot precharge pressure while changes in
accumulator volume had little effect. Variations in accumulator
entry line diameter or length affected transient pressure and
settling time. Increased valve snubbing reduced maximum transient
pressures.

x

DYNAMIC CHARACTERISTICS OF AERIAL

REFUELING SYSTEMS

I. Introduction

Problem Background

An aerial refueling system is an auxiliary pumping system installed
in a tanker aircraft which is used to transfer fuel to a receiver
aircraft. During inflight refueling operations fuel is pumped from
the tanker to the receiver through either an extensible, rigid
refueling boom or a flexible hose. Only the rigid boom method will be
considered in this study.

Fuel spillage during planned or inadvertent separation of the
tanker and receiver is prevented by use of a spring loaded shut-off
valve at the boom delivery nozzle. A spring loaded valve is also
provided at the receiver fuel receptacle.

The rapid closing of the nozzle shut-off valve during separation
can cause transient disturbances to propagate through the tanker
refueling system. Depending on the time interval of the transient,
pressure waves traveling at speeds close to that of sound waves,
about 3000 ft/sec, can easily generate energy enough to damage the
system. This is the so-called "waterhammer effect". Refueling
system performance enhancements such as higher fuel flow rates and
faster closing shut-off valves for less fuel spillage, can increase
the potential for damage due to transient pressure surges. Therefore,
pressure surge effects are of primary interest in the design of new
systems and the upgrading of existing configurations. For the

system structure to be maintained within aircraft weight standards and still withstand "worst case" pressure transients, methods must be employed to attenuate excessive pressure surges.

When designing surge attenuation components, reliable design data is needed to make a reasonable estimate of pressure surge magnitude. This design data is commonly obtained from either analytical studies, experiment, or both. General fluid transient phenomena have been researched and documented rather extensively. Wylie and Streeter (Ref 1) provide a comprehensive study of fluid transients and Goodson and Leonard (Ref 2) summarize the development of models for fluid line applications. Streeter and Lai (Ref 3) used numerical methods and the digital computer to solve waterhammer problems; their solutions were verified by experiment with good results. The McDonnell Douglas Corporation (Ref 4,5,6) used computer techniques to simulate complex aircraft and spacecraft hydraulic systems. Numerous experiments were performed to verify various test cases.

However, for aircraft refueling systems, there is a limited amount of well documented transient response experimental data. Some of the available experimental results have been used in extending the applications of existing hydraulic analysis programs to refueling systems. Parks and Franke (Ref 7) investigated modeling of the KC-135 tanker system. Their study focused on the transient conditions during and after a 0.05 sec closure of the nozzle shut-off valve. Kinzig et al. (Ref 8) studied the compatibility of the KC-135 and KC-10 tankers with a simulated receiver system. Shut-off valve closing times of approximately 0.22 and 1.0 sec were used to simulate

the receiver shut-off valve closures during refueling. The objective of the study was to predict transient pressures in the receiver aircraft.

Both of the refueling system simulations discussed above agreed favorably with experimental results for the conditions simulated. However, there is an element of uncertainty critical to all refueling system simulations that must be resolved to achieve accurate solutions. This element is the shut-off valve closure characteristics, i.e., valve area versus time. Kinzig (Ref 8:10) noted that small changes in closure curve shape could result in large differences in pressure surge magnitude. A McDonnell Douglas Corporation (Ref 9:6-7) laboratory test indicated nozzle valve closure times area function of separation rate. Thus, for varying separation rates of tanker and receiver the valve closure characteristics are likely to change. As a consequence, changes in separation rate will influence pressure surge magnitude. Therefore an accurate approximation of value closure characteristics is a critical input for refueling system simulations.

Scope and Objectives

The purpose of this thesis is to investigate, by computer simulation, the effects of variations in valve closure characteristics and surge attenuation components on the dynamic response of an aircraft refueling system. HYTRAN, a McDonnell Douglas Corporation (Ref 4) developed fluid transient analysis computer program will be used. Two distinct system configurations, the KC-135 and a preliminary KC-10 laboratory test set up, hereafter referred to as the Laboratory Test, will be modeled and simulated with the program.

The specific objectives of the study are to:

a) Establish an approximation of the actual valve closure characteristics for a typical refueling nozzle.

b) Verify the general utility of HYTRAN by comparison with results of Streeter and Lai.

c) Compare the simulated results of this study with experimental results of the Laboratory Test.

d) Determine, for the Laboratory Test model, the influence of variations in closure curve shape, i.e., valve area versus time, and modifications to surge attenuation components.

e) Determine, for the KC-135 model, the influence of both closure curve shape variation and closure time.

f) Examine the effect of varying the KC-135 surge boot precharge pressure.

II. System Description

General

Tanker aircraft are equipped to transfer fuel to receiver aircraft by means of an extensible, rigid boom or a flexible hose arrangement known as the probe and drogue system. This report considers only the rigid boom method. The refueling boom is basically a telescoping tube attached to the underside of the fuselage that is maneuvered into contact with a receiver aircraft. A nozzle at the end of the boom fits into a refueling receptacle on the receiver aircraft to provide a continuous flow path between the two aircraft. A spring-loaded poppet valve forms the seal in the end of the nozzle when the nozzle is not in contact with the receiver receptacle. The poppet valve is automatically opened during insertion of the nozzle into the receptacle by an actuator in the receptacle.

The primary surge attenuation component is the surge boot. A surge boot is an expandable, gas charged envelope that surrounds a perforated section of the boom, normally the aft portion. The basic parts of the surge boot are shown in Fig 1; the inner surface of the envelope seals the perforations in the boom until the fluid pressure in the boom exceeds the precharge on the gas. As the precharge is exceeded, fuel under pressure forces the envelope inner surface away from the outer surface of the boom. Therefore, fuel outflow through the perforations and into the cavity compresses the gas in the surge boot and provides energy dissipation during pressure surges.

During a normal disconnect of tanker and receiver a signal will be automatically sent through the system that shuts off the refueling
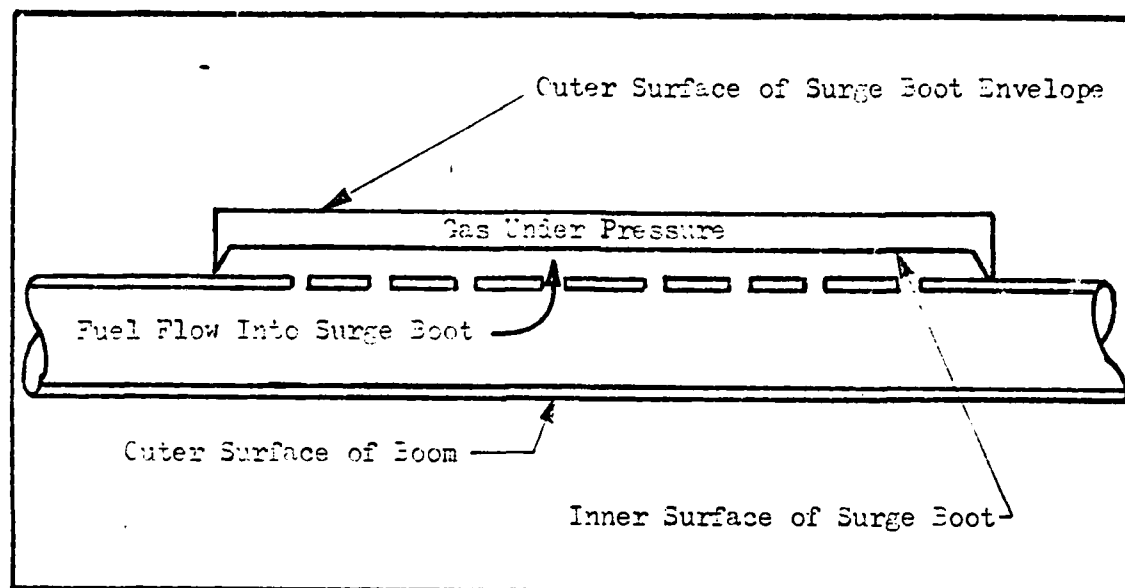
Fig 1. Surge Boot Details

pumps, opens a bypass valve, and initiates boom retraction. The opening of the bypass valve allows fuel to flow back to the tanker fuel tank so there is no sudden flow stoppage during disconnect and retraction. Any surge produced under these conditions will be mild and easily absorbed by the surge boot. Normal disconnects pose little or no threat to the system.

The abnormal disconnect conditions that cause concern are the breakaway situations due to turbulence, emergency actions, or a failure of the automatic process. In these cases it is likely that there will be a flowing disconnect whereupon the pumps continue to run against the closed shut-off valve in the nozzle with no retraction of the boom or bypass of the flow.

Failure of the pumps to shut-off increases the pressure in the line to deadhead pump pressure (in some cases 90 psia or more) in addition to any surge pressure induced by the nozzle shut-off valve

closure (Ref 11:6,16). Since no bypass of fuel occurs there is a stoppage of the full flow through the boom at the time of disconnect. High separation rates of the tanker and receiver, up to the normal maximum of 6.5 ft/sec (Ref 9:7), are usually associated with abnormal disconnects.

KC-135 System (Ref 11,12)

A simplified diagram of the KC-135 refueling system is shown in Fig 2. The KC-135 refueling system is a four pump (constant rpm, each rated at 300 gpm @ 80 psig) system with two refueling pumps in the forward body tank and two in the aft body tank. Reverse flow is prevented to each pump by individual check valves. Fuel flows from all four pumps are united in a main trunk line; fuel then flows through a shut-off valve, pressure regulator, and venturi. Finally the fuel flows through the boom which contains a surge boot with a nominal precharge of 50 psig. The pressure regulator is set to maintain the steady state pressure at the nozzle to 50 ± 5 psig. A secondary method of pressure surge protection is provided by two level control valves located in the lines leading from the refueling manifold to the forward and aft body tanks. The valves' cracking pressure of 85-115 psi allows fuel to flow to the body tanks during pressure surges (Ref 10:3).

Laboratory Test

The McDonnell Douglas Corporation performed an experimental investigation (Ref 9) to study surge pressures developed by the closure of shut-off valves during tanker/receiver disconnects. These

7

Refueling
Pump #1

To Forward Body Tank

Level Control Valve

Checkvalves

Refueling
Pump #2

Ground Refueling Port

Refueling
Pump #3

Checkvalves

Refueling Manifold

Refueling
Pump #4

Level Control Valve

Line Valve

To Aft Body Tank

Regulator

To Aft Body Tank

Bypass Valve

Vacuum Relief

Venturi

Boom Inlet

Surge Boot

Boom Nozzle
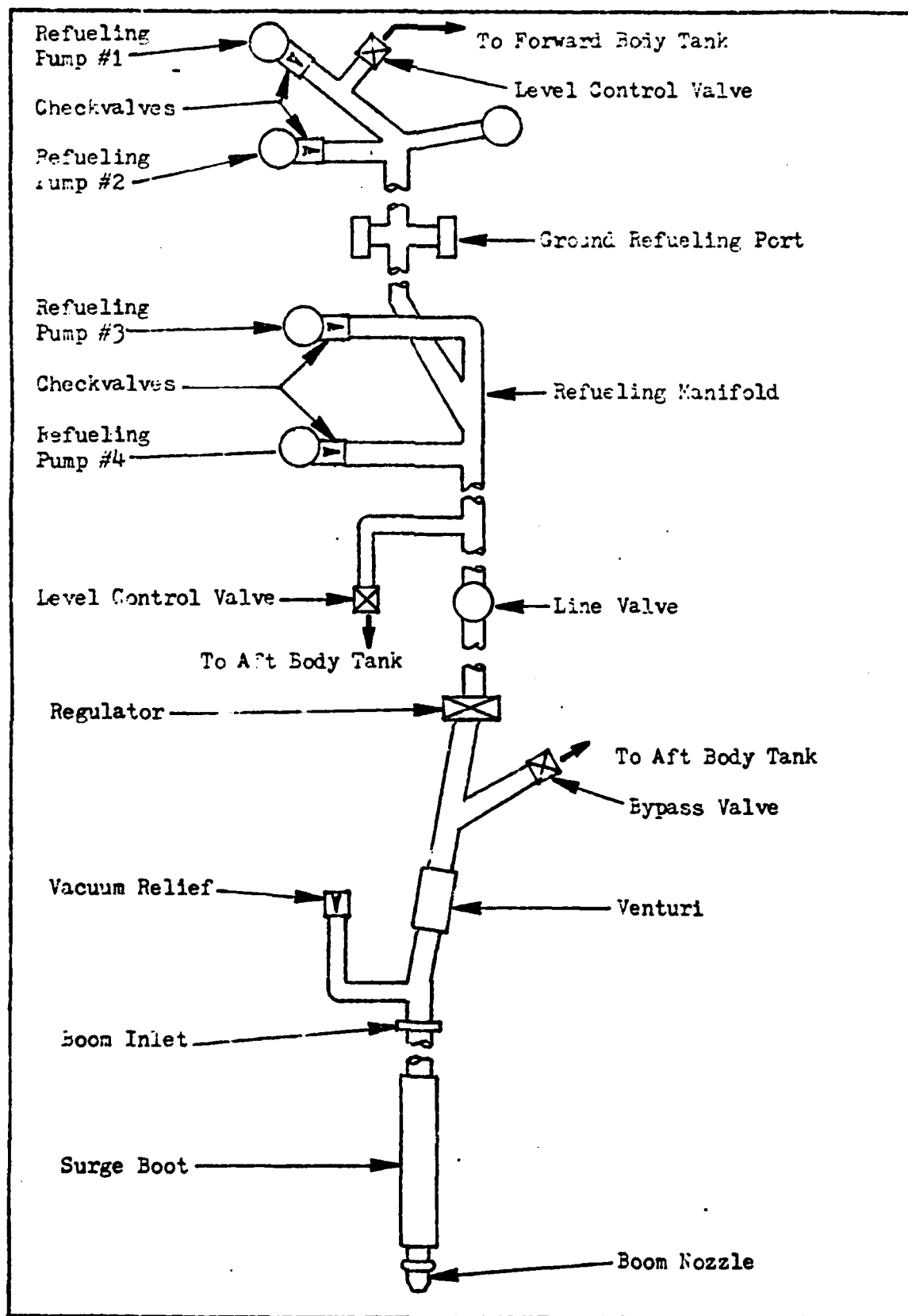
Fig 2. Simplified Diagram of KC-135 Refueling System

tests were performed as part of the Advanced Aerial Refueling Boom/ Advanced Aerial Refueling Nozzle development program proceeding the KC-10 development.

The experimental setup shown in Fig 3 consisted of an aluminum tube assembly simulating the actual refueling boom, four discrete accumulators to simulate the surge boot, and a laboratory pumping system that supplied fuel to the rig. A refueling nozzle was mounted at the end of the aluminum tube and a refueling receptacle was attached to a carriage that was free to slide between two tracks. The receptacle separation was driven by means of a hydraulic and bungee system.

The test procedure was to establish a predetermined flow rate, set the load on the receptacle for the anticipated separation rate, and activate the disconnect system. Data recorded included flow rate, boom inlet and nozzle pressure, separation rate, and nozzle valve poppet travel. The test conditions are discussed in Chapter IV with the computer simulation model description.

Fig 3. Laboratory Test Configuration

Refueling Receptacle mounted on carriage

Refueling Boom Nozzle

5.30 in OD
5.05 in ID

2 in OD
1.75 in ID
6 in long } approx.

Gas Charged Accumulators

Aluminum Tubing (both sections)
5.00in OD
4.75in ID

Boom Inlet

JP-5 from Laboratory Pumping System

647 in

314 in

300 in

36 in

86 in
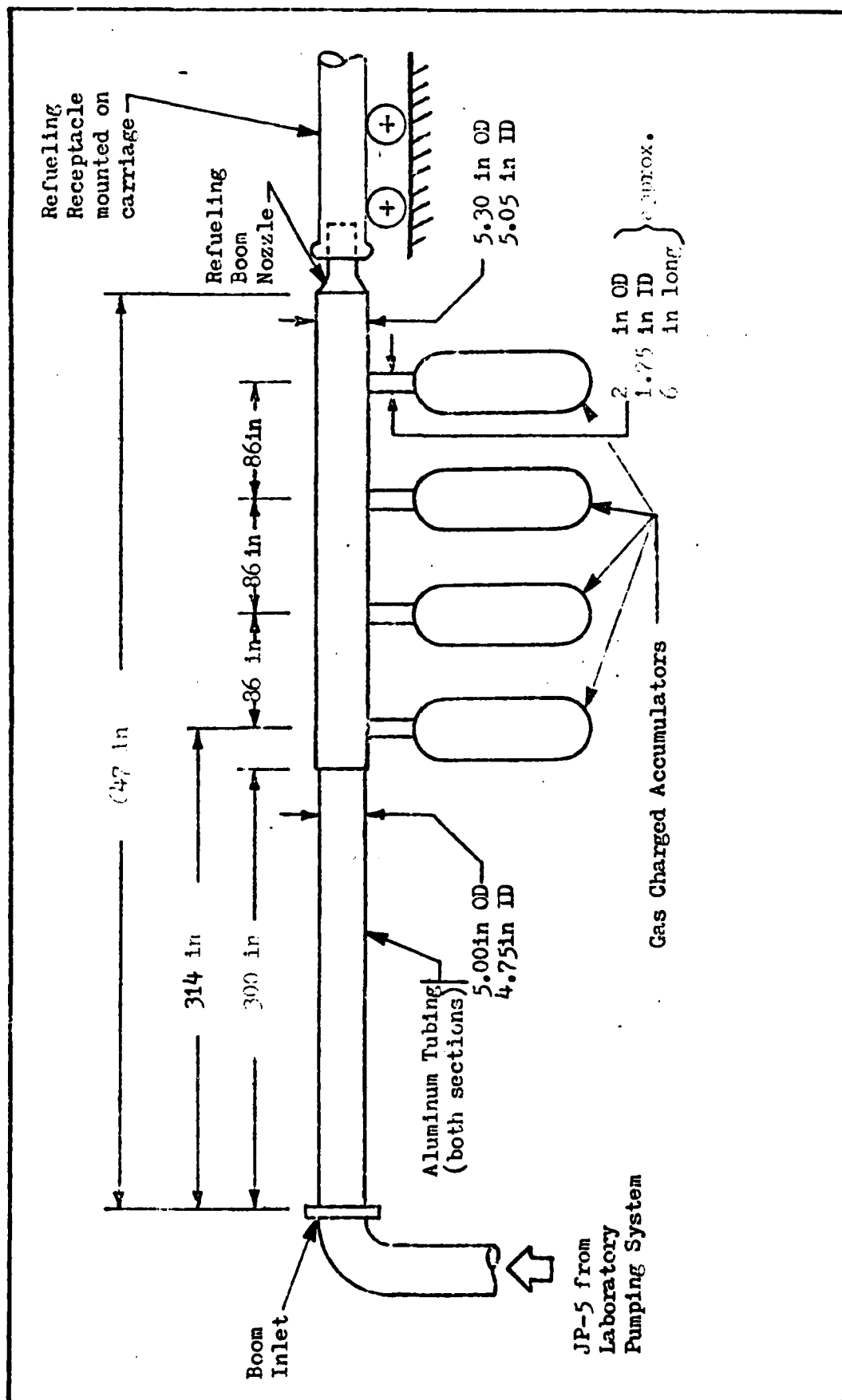
86 in

III. Computer Program Description

General

HYTRAN, the hydraulic transient analysis computer program used in this study, was developed by the McDonnell Douglas Corporation under an Aero Propulsion Laboratory contract (Ref 4). The contract included not only program development but also extensive validation and documentation. The program uses a building block approach to facilitate simulation of complete systems. After the configuration is established according to HYTRAN format, the program calculates the values of flows, pressures, and component variables throughout the system.

The basic theory of HYTRAN is that a change in flow (momentum) results in a change in pressure. Flow is brought to rest at the expense of an increase in pressure. By coupling the continuity and momentum equations with component equations, pressure and flow as a function of time and line distance can be determined. The mathematical solution technique used by the program is the method of characteristics. The major assumptions upon which the program is based are:

a) Fluid temperature is held constant during the entire run.

b) Flow is one dimensional, that is, the fluid properties are constant across any transverse cross section of pipe.

c) Pipes have circular cross sections and friction factors based on smooth, drawn tubing.

d) Stresses in pipes are always below the elastic limit.

11

e) Pipe geometry is such that the "thin wall" case is valid.

f) Pipe and liquid are perfectly elastic (all energy dissipation is due to shearing stresses at the walls).

Each component subroutine has its own set of assumptions since each model is broken down into its most basic equations of motion and flow.

The controlling input to the system is normally a valve motion, which causes a disturbance to propagate through the system at or near the speed of sound. The components of the system each have a response to the pressure and flow changes.

HYTRAN is composed of four basic parts: input, steady state calculations, transient calculations, and output. A simplified flowchart is shown in Fig 4.

Included in the input data are line and component parameters, the system configuration, i.e., how the lines and components are connected, initial conditions, fluid properties, and various directive parameters such as time steps, run time, plotting intervals, etc.

The steady state section of the program balances the pressures and flows in the system and calculates the initial values for all the system variables. Once the initial values are established at zero time, the program starts by calculating, for a small change in time (ΔT), new flows, pressures, and values for the component variables such as valve position, accumulator fluid volumes, etc.

The program continues forward in ΔT time intervals, first calculating the line and then the component variables until the desired simulation time period is covered.

The output is time histories of selected system variables which

12
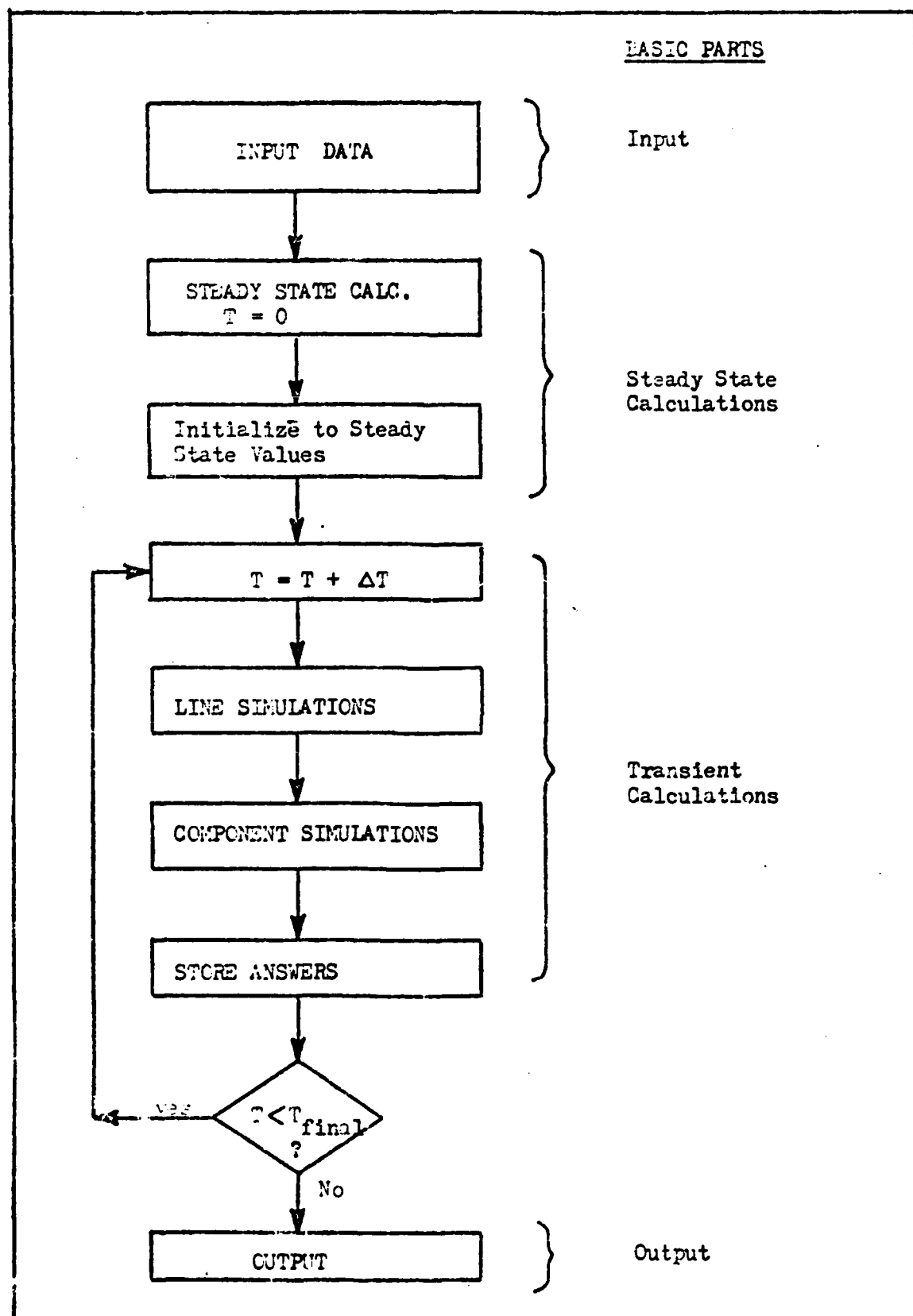
Fig 4. Simplified HYTRAN Flowchart

have been disturbed by the controlling input. A typical output plot
would be a pressure versus time curve for before, during, and after
a valve closure.

A detailed description of program structure, methods of solution
and component models is provided in Ref 4. The program requires
approximately 170,000 core memory and a run time between 80 and 300 sec.

Fuel System Usage

Although HYTRAN was developed for use with hydraulic systems, the
basic assumptions and solution techniques are common to most fluid
systems. The main alterations required for use with fuel systems
was to change the fluid properties from hydraulic fluid to fuel.

System Modeling

The first step in developing a HYTRAN model is to construct the
system schematic in HYTRAN format. This involves the assignment of
line, component, node, and leg numbers throughout the system as well
as determining which component models will be selected to simulate
each individual component. References 13 and 14 explain in detail how
to translate a system into HYTRAN format.

The specific HYTRAN component models used for the simulation
models discussed in Chapter IV and V are discussed briefly in the
following paragraphs. Detailed descriptions of each component model
can be found in Ref 4 and 15.

Fuel tanks and flow sources were simulated with HYTRAN TYPE 61
constant pressure reservoirs. The reservoir is assumed to have an
infinitely large gas volume so that pressure remains unchanged.

Lines were joined at branches and junctions with HYTRAN TYPE 11 branches. The branches do not incorporate any losses associated with changes in diameter and flow direction or divisions, i.e., they are frictionless branches.

Fixed orifices were modeled using HYTRAN TYPE 41 restrictors. The model assumes flow in either direction. The discharge coefficient is the same for flow in each direction and constant over the entire flow regime.

The HYTRAN TYPE 31 check valve model was used to simulate check and relief valves. The check valve is modeled as an orifice of variable area. The area at any given time is determined by the position of the force-balanced poppet. Reverse flow can take place until the valve closes.

Control valves were simulated using HYTRAN TYPE 21 two-way valves. The valve is modeled as an orifice of variable area and a constant discharge coefficient over the entire flow range. A time history of valve closure is input in the form of an effective valve area versus time table. The effective valve is defined as the valve area at a particular time multiplied by the discharge coefficient. In this study, valve area versus time plots are presented in the nondimensional form of valve position versus percent of closure time. The valve position, given in percent open, is the valve area with respect to the full flow valve area. Likewise, the percent of closure time values are the time values for each valve position with respect to the total closure time. Therefore, the effective area with respect to time for program input is obtained by multiplying the full flow area by valve position and discharge

coefficient is shown below

$$A_v(t) = K(t)C_d A_{vo} \tag{1}$$

where

$A_v(t)$ = effective valve area with respect to time

$K(t)$ = valve position with respect to time

C_d = discharge coefficient

A_{vo} = full flow valve area

Accumulators were simulated with HYTRAN TYPE 71 accumulator models. Each unit is modeled as a simple gas charged piston type accumulator with the frictional and inertial effects neglected. The model assumes a nonvarying gas constant and no heat transfer between the gas and the accumulator walls.

IV. Laboratory Test Computer Model

The Laboratory Test configuration in Fig 3 was modeled using the HYTRAN components discussed in Chapter III. A schematic of the test configuration in HYTRAN input format is shown in Fig 5.

Input data for all lines except those entering the accumulators were obtained from the Laboratory Test report (Ref 9). The outside diameter of the accumulator entry lines was not available and was estimated from measurements of test rig photographs. An assumed inside diameter was based on the thickness of other tubing used in the experiment.

Fluid properties were altered from hydraulic fluid to those of JP-5 at 60 F. The properties used were:

$$\text{Viscosity} = 0.0362 \times 10^{-2} \text{ in}^2/\text{sec}$$

$$\text{Density} = 0.720 \times 10^{-4} \text{ lb}_f\text{-sec}^2/\text{in}^4$$

$$\text{Bulk Modulus} = 0.189 \times 10^6 \text{ lb}_f/\text{in}^2$$

$$\text{Vapor Pressure} = 0.5 \text{ psia}$$

Time steps (ΔT) of 0.0005, 0.0004, and 0.000333 sec were used over a simulation interval of 0.4 sec. This interval was chosen to match the time period over which the experimental data were recorded. The various time steps were used, when required, to insure a whole number of time steps over all segments of each of the effective valve area versus time input tables.

The nozzle was modeled using a TYPE 21 two-way valve. The valve closure was input as an effective valve area versus time as discussed
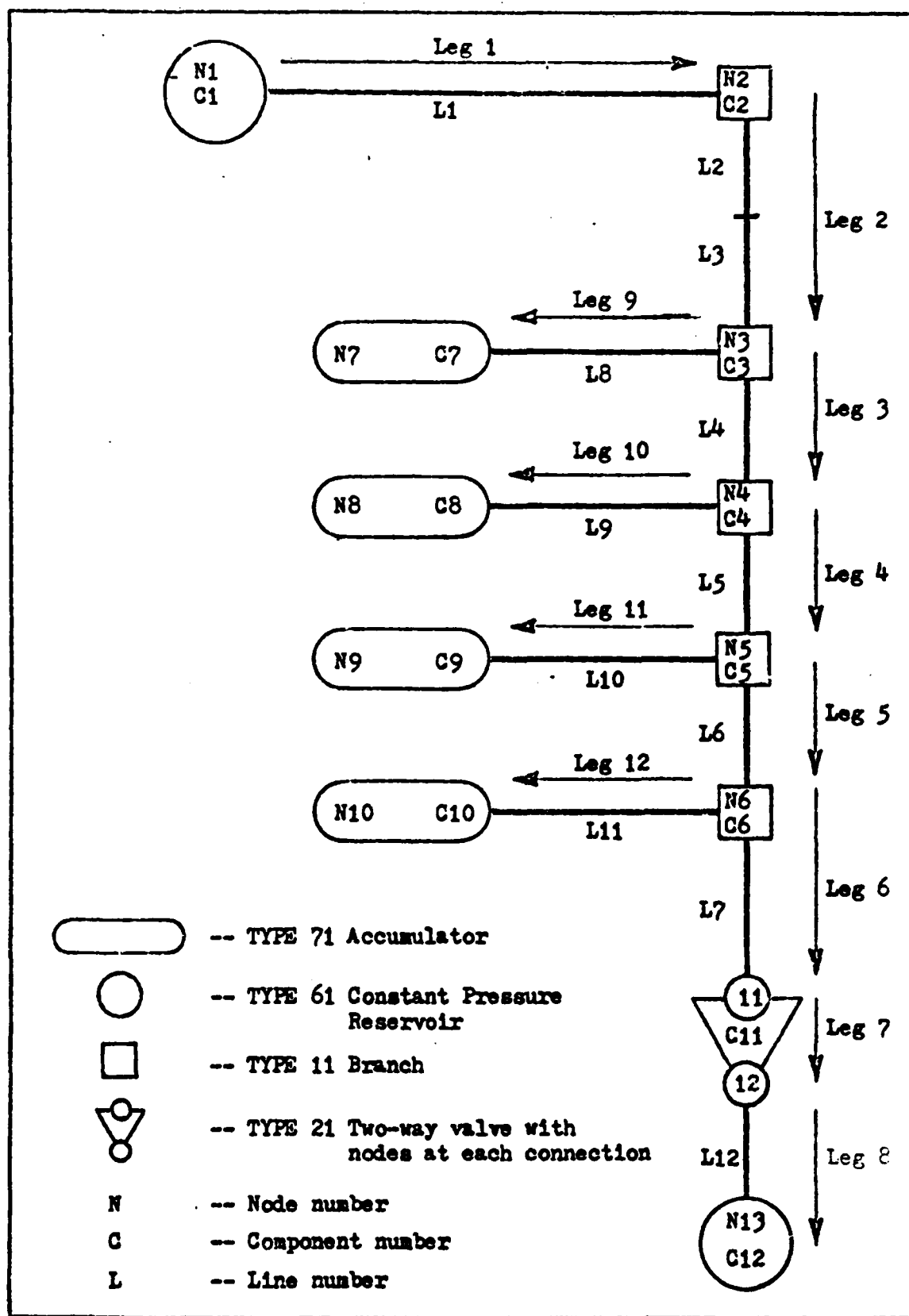
Fig 5. HYTRAN Diagram of Laboratory Test

Legend:
- TYPE 71 Accumulator
- TYPE 61 Constant Pressure Reservoir
- TYPE 11 Branch
- TYPE 21 Two-way valve with nodes at each connection
- N — Node number
- C — Component number
- L — Line number

in Chapter III. This method simplified modifications and the usage of various closure curves.

The full flow area times discharge coefficient was calculated from a flow versus pressure difference across the nozzle curve for the actual nozzle (Ref 16:44). A flow rate of 2018 in^3/sec was used in the Laboratory Test. This flowrate corresponds to $\Delta P = 5.1$ psi from the curve for the nozzle. Using the orifice equation,

$$A_{vo}C_d = \frac{Q}{\sqrt{\frac{2\Delta P}{\rho}}} \tag{2}$$

a steady state value of $A_{vo}C_d = 5.35$ in^2 was computed.

The steady state flow was exhausted into a TYPE 61 constant pressure reservoir to simulate the fuel return system used in the test. The constant pressure was set at 47.5 psia. This pressure was computed by subtracting the ΔP of the nozzle from the measured steady state flowing pressure of 52.6 psia just upstream of the nozzle (Node 11). This back pressure was consistent with the conditions used to generate the flow curve for the nozzle.

TYPE 71 gas charged accumulators were used to simulate the test accumulators. Volume and precharge pressure was the only definitive data available for the accumulators; therefore, some assumptions were required to complete the models. Entry lines were scaled from photographs to be 6 in long with an outside diameter of 2 in. A wall thickness of 0.125 in was assumed. The volume of each accumulator was given as 5 gal (1155 in^3); a usable volume of 1000 in^3 was used in the simulation to account for the unknown

19

internal configuration. Assuming that the gas would be compressed to a maximum of ten percent of its original volume resulted in a maximum fuel volume for each accumulator of 900 in^3. The total fuel volume for the four accumulators totaled 3600 in^3, consistent with the actual volume of 3565 in^3 (Ref 17) for the KC-10.

No data other than photographs was available for the Laboratory pumping system. Since the system provided a constant steady state flow and pressure, a TYPE 61 constant pressure reservoir was used to model the pump as a constant pressure source. The pressure of the reservoir was adjusted to provide the test condition steady state flow.

A complete listing of input parameters for the Laboratory Test model is given in Appendix A.

V. KC-135 Computer Model

The KC-135 system was modeled using the technique of Parks
(Ref 10) and the HYTRAN component models discussed in Chapter III.
The use of a similar model and test conditions provided a cross-check
and extension of the previous results. Although Parks used an
earlier version of HYTRAN which required recomputation of some input
parameters, the basic model configuration was unchanged. A schematic
of the system in HYTRAN format is shown in Figures 6 and 7.

Fluid properties were altered from hydraulic fluid to JP-4
at 60 F. The properties used were:

$$\text{Viscosity} = 0.136 \times 10^{-2} \text{ in}^2/\text{sec}$$

$$\text{Density} = 0.77 \times 10^{-4} \text{ lb}_f\text{-sec}^2/\text{in}^4$$

$$\text{Bulk Modulus} = 0.16 \times 10^{-6} \text{ lb}_f/\text{in}^2$$

$$\text{Vapor Pressure} = 2.0 \text{ psia}$$

Time steps (ΔT) of 0.0005, 0.0004, and 0.000333 sec were used
over a simulation interval of 1.0 sec. This interval was
selected to match Parks' simulation time interval (Ref 10:23).
The various time steps were used, when required, to insure a whole
number of time steps over all segments of the valve closure input
tables.

Parks simulated the KC-135 system with three pumps on and one
pump off (Ref 10:23); this study used the same configuration to
facilitate comparisons with Parks. Each pump was modeled as a TYPE
61 reservoir at a constant pressure of 30 psig. Pump check valves
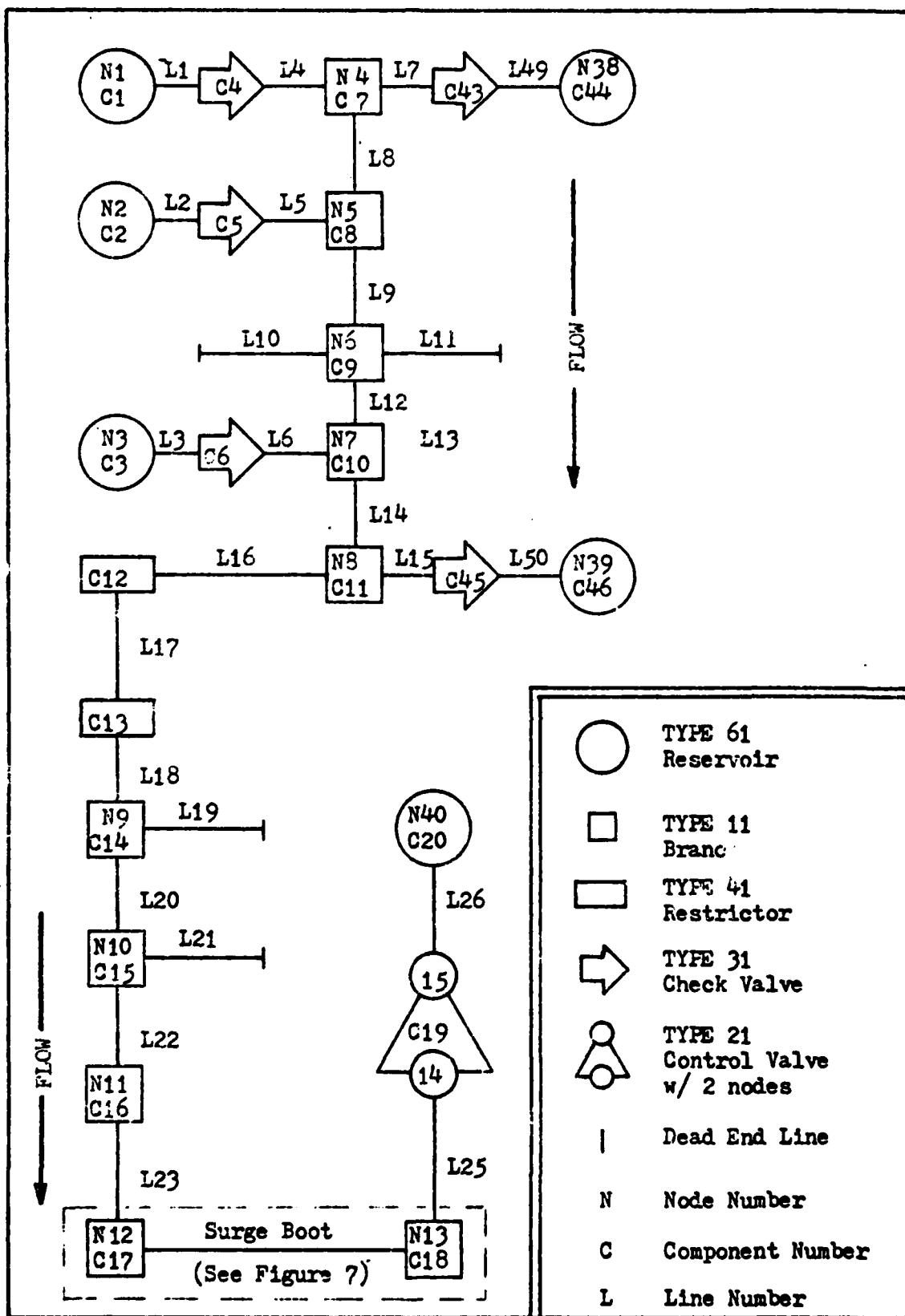
Fig 6. HYTRAN Schematic of KC-135 Refueling System

N30 C36 L39 | N19 C24 | L31 | N20 C25 | L46 | N31 C37

L30

L32

N29 C35 L45 | N18 C23 | N21 C26 | L40 | N32 C38

L29

L33

N28 C34 L38 | N17 C22 | N22 C27 | L47 | N33 C39

L28

L34

N27 C33 L44 | N16 C21 | N23 C28 | L41 | N34 C40

L27

L35

N26 C32 L37 | N37 C30 | N24 C29 | L48 | N35 C41

L24

L36

N25 C31 L43 | N12 C17 | N13 C18 | L42 | N36 C42

L23   FLOW   L25

| TYPE 71 Accumulator | TYPE 11 Branch | N – Node Number C – Component Number |

Fig 7. HYTRAN Schematic of KC-135 Surge Boot

were simulated as TYPE 31 checkvalves.

The line valve and regulator were modeled as TYPE 41 restrictors; the level control valves as TYPE 31 checkvalves and the fuel tanks as TYPE 61 reservoirs, respectively. The surge boot was modeled as twelve discrete accumulators; the total volume of the twelve units was 1300 in^3. Each was modeled as an individual TYPE 71 accumulator with a minimum gas volume equal to ten percent of the initial gas volume.

A TYPE 21 control valve was used to simulate the boom nozzle. The valve closure was input as an effective valve area versus time as discussed in Chapter III.

All dimensions, where applicable, were obtained from the Parks model (Ref 10:70-77).

The steady state flow was exhausted into a TYPE 61 reservoir to simulate the fuel return system. The reservoir pressure was set to 43 psig (Ref 10:36).

A complete listing of input parameters can be found in Appendix B.

VI. Discussion of Valve Closure

General (Ref 17:69)

As discussed in Chapter I, a nozzle valve closure causes a
pressure surge to propagate through a refueling system. The direct
relationship of pressure surge magnitude to valve closure can be
illustrated by considering the deceleration of an incompressible
fluid flowing frictionlessly in a rigid pipe of uniform area A with
a velocity V. The pipe has a length L, an inlet pressure P_1, and
a pressure P_2 at L. Assume, at length L, there is a valve which can
reduce the velocity at L to $V - \Delta V$. The mass rate of flow for a
pressure wave traveling at sonic velocity c, is $\dot{m} = \rho Ac$. From the
impulse-momentum equation, for this application

$$(\rho Ac)(V - \Delta V - V) = P_2 A - P_1 A$$

or the increase in pressure is given by

$$\Delta P = -\rho c \Delta V \tag{3}$$

thus a change in velocity is directly proportional to a change in
pressure. The time for a pressure wave to travel the length of
pipe L and return is $t = 2L/c$. If the time of closure T_c is less
than or equal to t, the approximate pressure rise is given by

$$\Delta P \approx \frac{-2 \rho VL}{T_c} \tag{4}$$

thus a decrease in closure time will cause an increase in pressure rise.

Since the reduction in flow velocity is determined by the valve closure, it is apparent that the closure curve is a critical input to the simulation of aircraft refueling system response subsequent to nozzle valve closures.

Valve Closures from Previous Research

Parks (Ref 10:19-20) used a valve closure relationship, hereafter referred to as curve "A", described by Eq (1) where

$$K(t) = \left[1 - \frac{t}{T_c} \right]^3 \tag{5}$$

The closure curve corresponding to this relationship is shown in Fig 8 and is characterized by a rapid reduction of the valve opening initially, followed by an almost asymtotic reduction to full closure. This slower area reduction during the final stage of the closure curve is referred to as "valve snubbing". Parks justified his usage of the curve on the basis of a comparison to experimental data.

Typical curves used by Kinzig (Ref 8:25) in his study of receiver pressure surges are shown in Fig 9.

For use in this study, the curves were reduced to an analytical expression of the following form:

Fig 8. Closure Curve 'A'
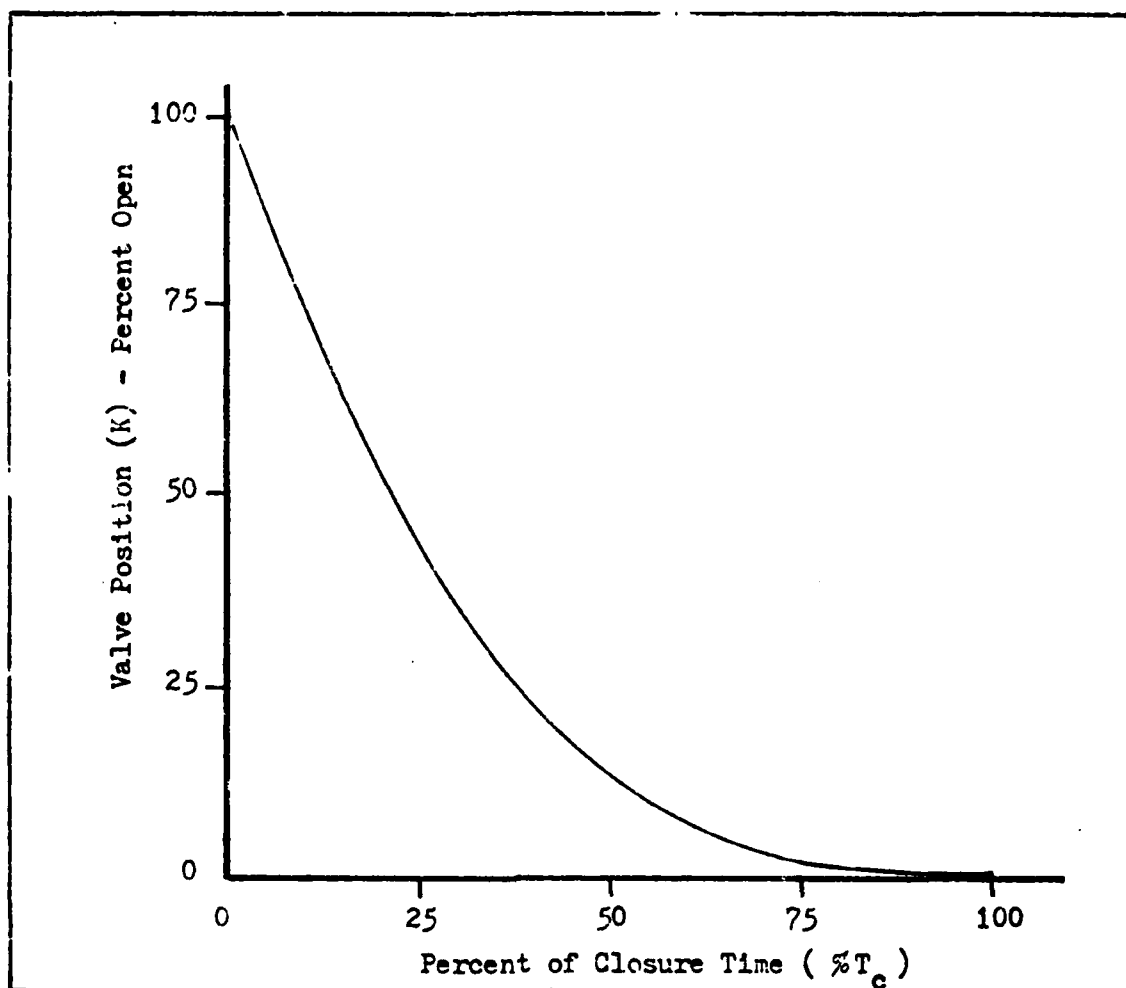
$$K(t) = \left[1 - (t / T_c) \right]^{\left[a - b(1 - (t / T_c)) \right]^{(n)}} \qquad (6)$$

where for   curve "B"   curve "C"

          a = 1.45   a = 2.60

          b = 1.00   b = 2.00

          n = 1.30   n = 1.25

Both curves represent a relatively gentle closure characteristic
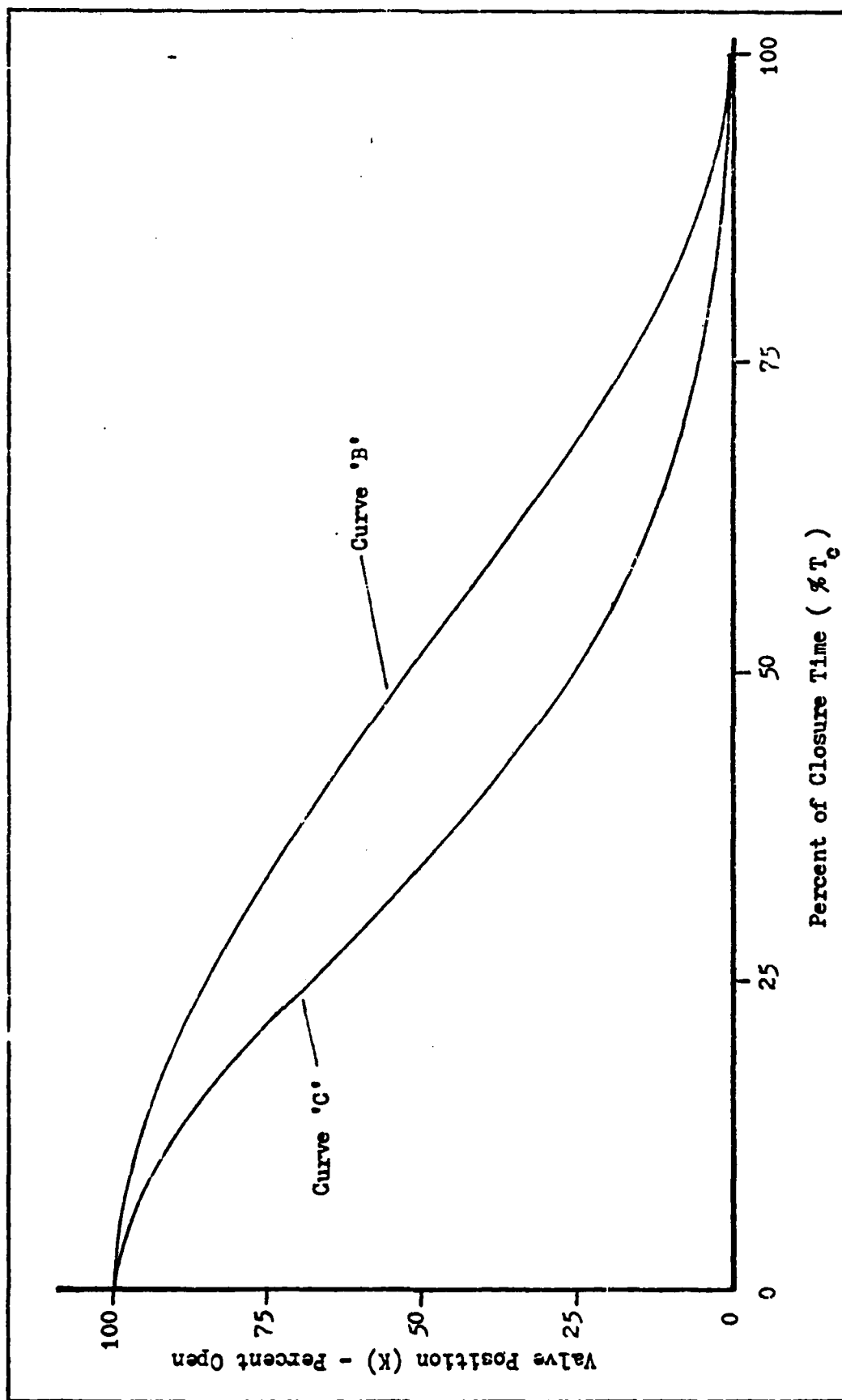of receiver shut-off valves.

Fig 9. Closure Curves 'B' and 'C'

Nozzle Valve Closure

Valve poppet position versus time from the Laboratory Test (Ref 9:24) and drawings of the valve mechanism were used to plot an actual closure curve for a refueling nozzle. The curve, in nondimensional form, is shown in Fig 10. From fully open, the valve closes at an increasing rate as it accelerates to a constant closure rate. The closure rate decreases during the final stage of area reduction, approximately the last ten percent. This snubbed closure is expected since the valve poppet incorporates a damper that is designed to slow the closure during the last stage of poppet travel.

Nozzle / Receptacle Combination

While the previous curves, Figs 8 and 9, may be typical for normal disconnects, abnormal disconnects at high separation rates are likely to result in more severe closures. Before establishing the effect of high separation rates on the valve closure curve, the interaction of the combined nozzle and receptacle configuration was examined.

Shown in Fig 11 are (a) the receptacle sleeve valve, (b) the nozzle valve, (c) the nozzle and receptacle in connected position. The spring-loaded nozzle poppet valve is opened mechanically on contact with the fixed pedestal in the receiver aircraft receptacle in conjunction with the opening of the sliding sleeve valve in the receptacle by the nozzle tip.

During quick disconnects, the damper in the poppet can slow the poppet closure such that the poppet and pedestal do not remain in contact during separation of the nozzle and receptacle. Therefore, nozzle valve closure is independent of separation rate. Conversely,
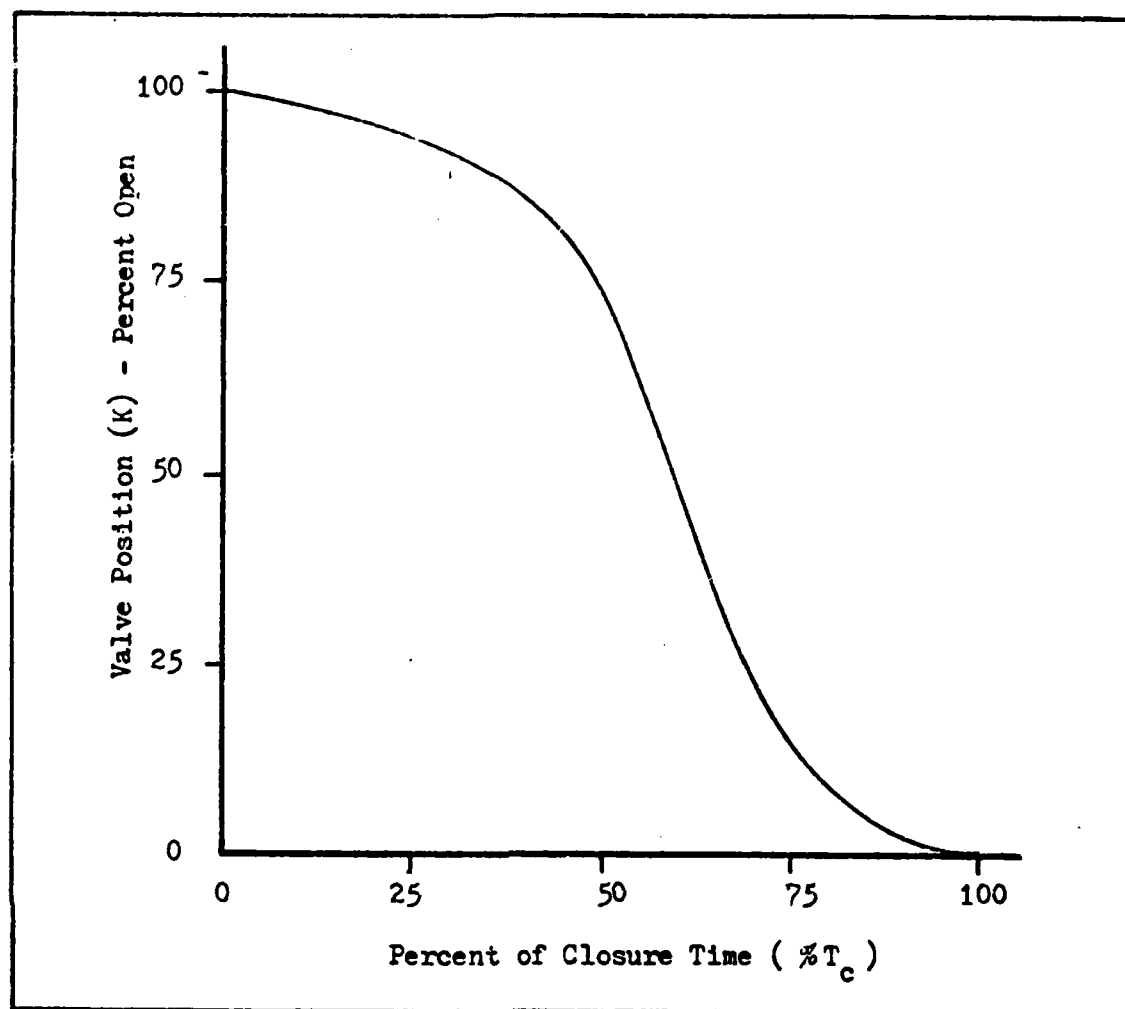
Fig 10. Nozzle Closure Curve Computed from the
Laboratory Test Measurements

since the receptacle sleeve valve is spring-loaded and undamped, its

closure rate is determined by the rate of separation. A typical closure

curve for the receptacle sleeve valve, hereafter referred to as curve

"D", is shown in Fig 12. The closure accelerates to a constant rate

with no appreciable snubbing.

To reach the fully closed position, the required travel for the

receptacle sleeve valve is 1.0 in (Ref 9:7) and for the nozzle valve

poppet a minimum of 1.15 in is required to reach the closed position

(Ref 16:50). Therefore, when the nozzle and receptacle have separated

One inch of travel required to close Sleeve Valve

Sleeve Valve in open position

Pedestal

Sleeve Valve in closed position

(a) Receptacle Sleeve Valve

1.15 in

Poppet Valve in closed position

Spring-loaded Poppet

Poppet Valve in open position

(b) Nozzle Valve

Fuel Flow

Nozzle Valve depressed by Pedestal

(c) Nozzle and Receptacle in Connected Position
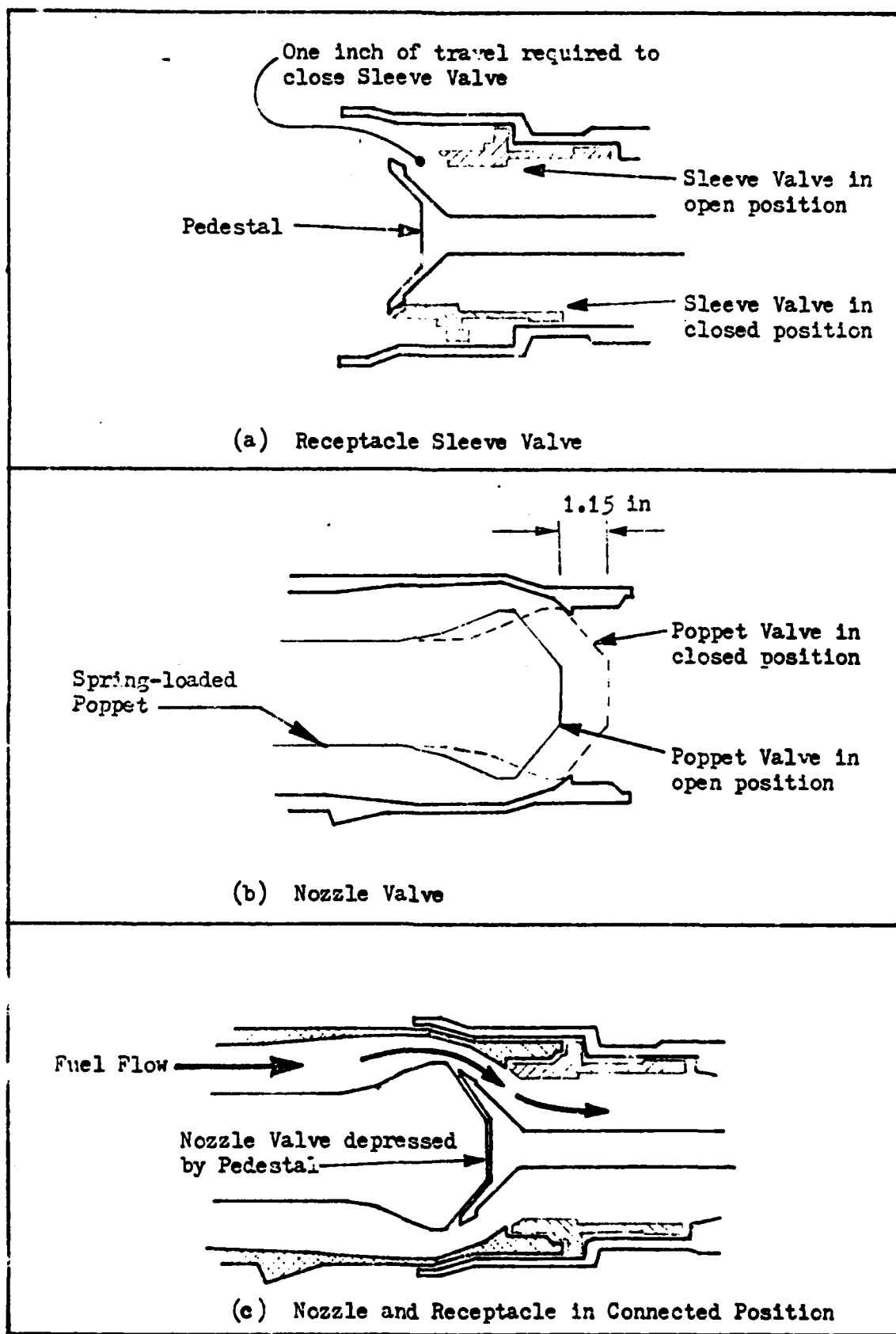
Fig 11. Nozzle / Receptacle Details

41
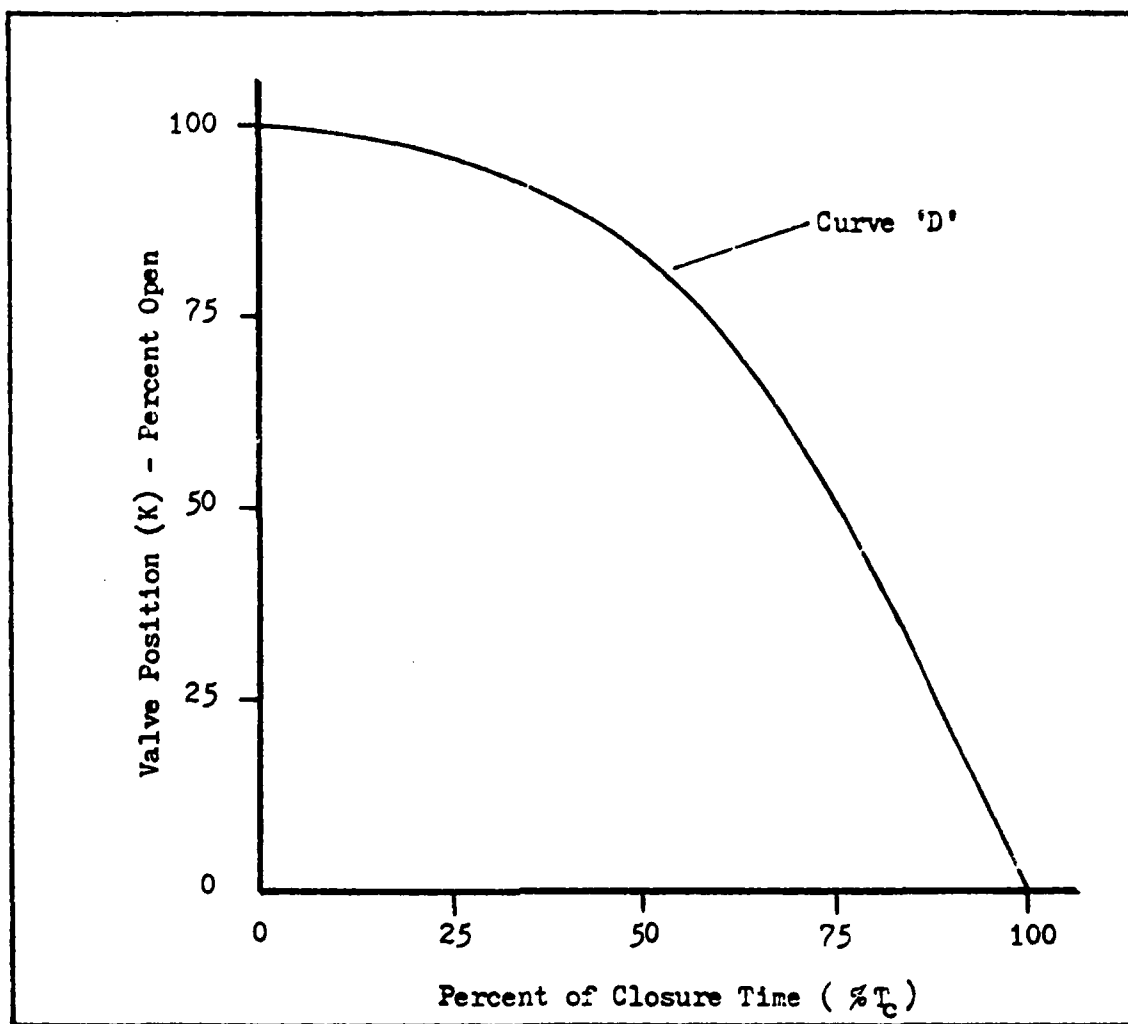
Fig 12. Receptacle Closure Curve

1.0 in, Fig 13, the receptacle sleeve valve is closed. At the 1.0 in separation point the nozzle valve has reached a maximum of approximately 90% of full closure if the poppet and pedestal have remained in contact, less if the poppet travel lags the relative separation of the two components. The penetration of the nozzle into the receptacle is sufficient for the two components to be essentially sealed together at this position of separation. The actual closure for quick disconnects is determined by the receptacle sleeve valve and can initiate a surge that propagates into the tanker
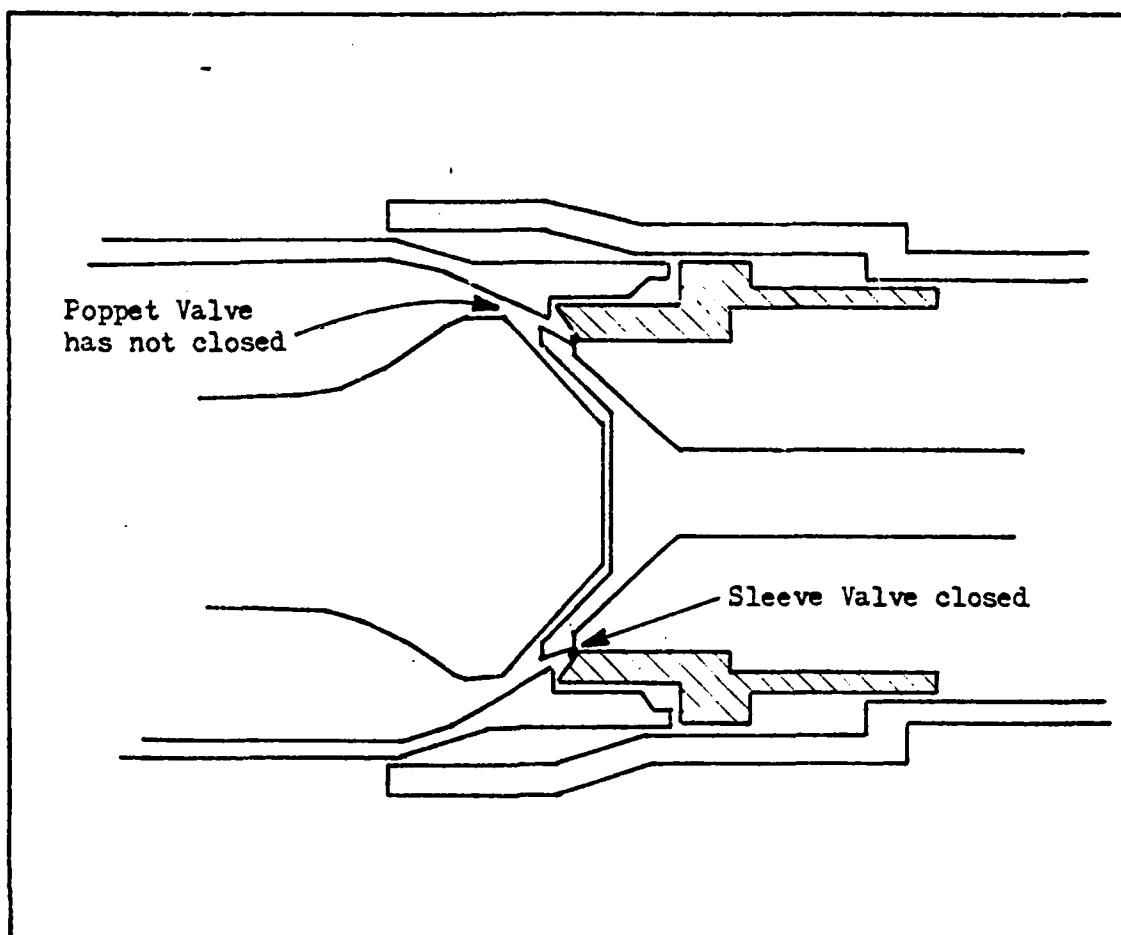
Fig 13. Nozzle and Receptacle at the One Inch
Separation Point

system even though the nozzle valve is still open. This supposition

is supported by pressure measurements obtained during the Laboratory

Test (Ref 9:10) which indicate peak pressure occurs coincident with

the 1.0 in separation point for separation rates of 5-10 ft/sec.

Actual Valve Closure Approximation

With a relationship between separation rate and valve closure

established, a reasonable approximation to the minimum effective

closure time can be established. The maximum disconnect speed is

6.5 ft/sec (Ref 9:7). Assuming instantaneous acceleration to this

rate, the time required for the nozzle and the receptacle to separate
one inch is 0.013 sec. The separation rates measured during the
Laboratory Test (Ref 9:10) indicate a minimum time for one inch
separation of approximately 0.02 sec at a separation rate of 6 ft/sec.

Based on the previous discussion in this chapter the closure
curve for quick disconnects is theorized to be basically the
receptacle closure curve as shown in Fig 12 (curve D). Typically the
closure rate would increase to a constant rate with no snubbing. The
overall effect of the combined nozzle/receptacle closure is to
eliminate the snubbing portion of the closure action of the
receptacle.

VII. Results and Discussion

HYTRAN Verification

A basic waterhammer problem with known results was solved using HYTRAN. Streeter and Lai (Ref 3) obtained an analytical solution for the configuration shown in Fig 14 and verified it by experiment. After establishing a steady state flowrate in the line, the valve was closed according to Eq (1) where

$$K(t) = \left[1 - \frac{t}{T_c} \right]^2 \tag{7}$$

The HYTRAN format configuration is shown in Fig 15. A closure time of 0.09 sec and a steady state flowrate of 5 in^3/sec was used. The working fluid was water at 60 F.

Comparison of HYTRAN and Streeter results (Fig 16), indicate excellent agreement in phasing, curve shape, and magnitude of the first peak. Subsequent peaks of the HYTRAN solution exhibit more attenuation than the Streeter solution due to the inclusion of dynamic friction effects in HYTRAN that Streeter neglected.

Laboratory Test Simulation

Comparison with Experimental Results. The steady state conditions prior to the separation of nozzle and receptacle, i.e., valve closure, were as described in Chapter IV. The accumulator precharge was set at 90 psia (Ref 9:10, 24). The valve was closed
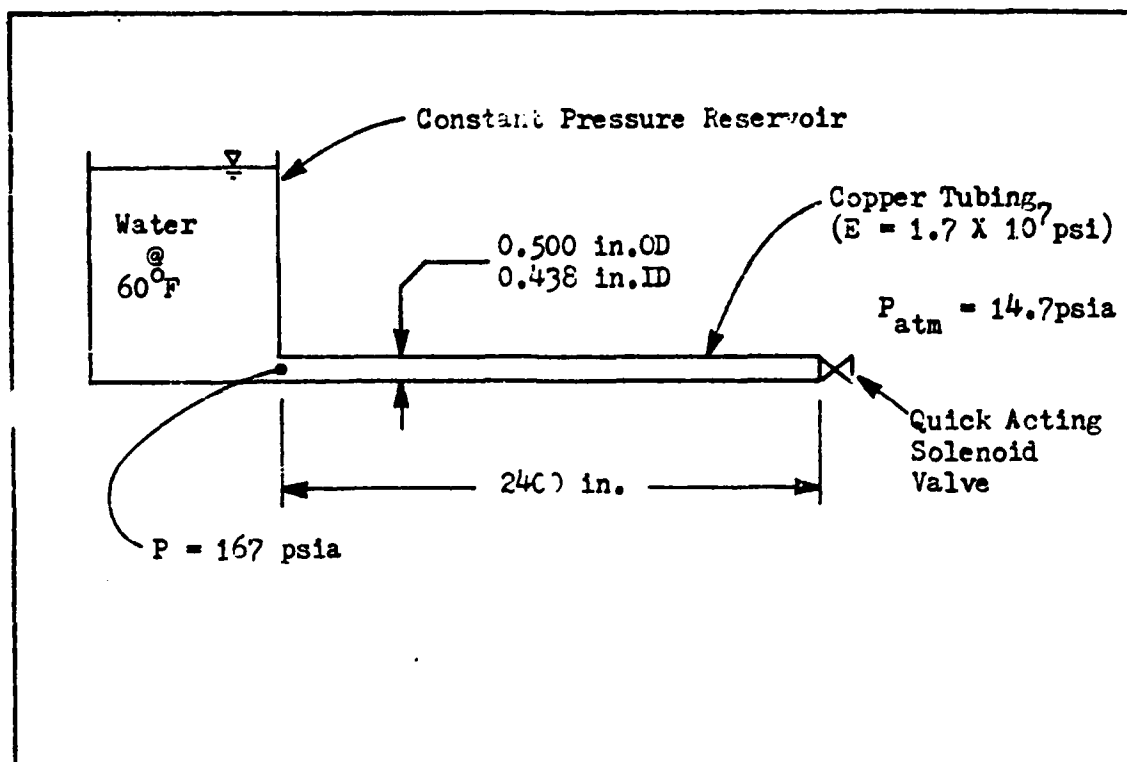
Fig 14. Streeter's Experimental Configuration

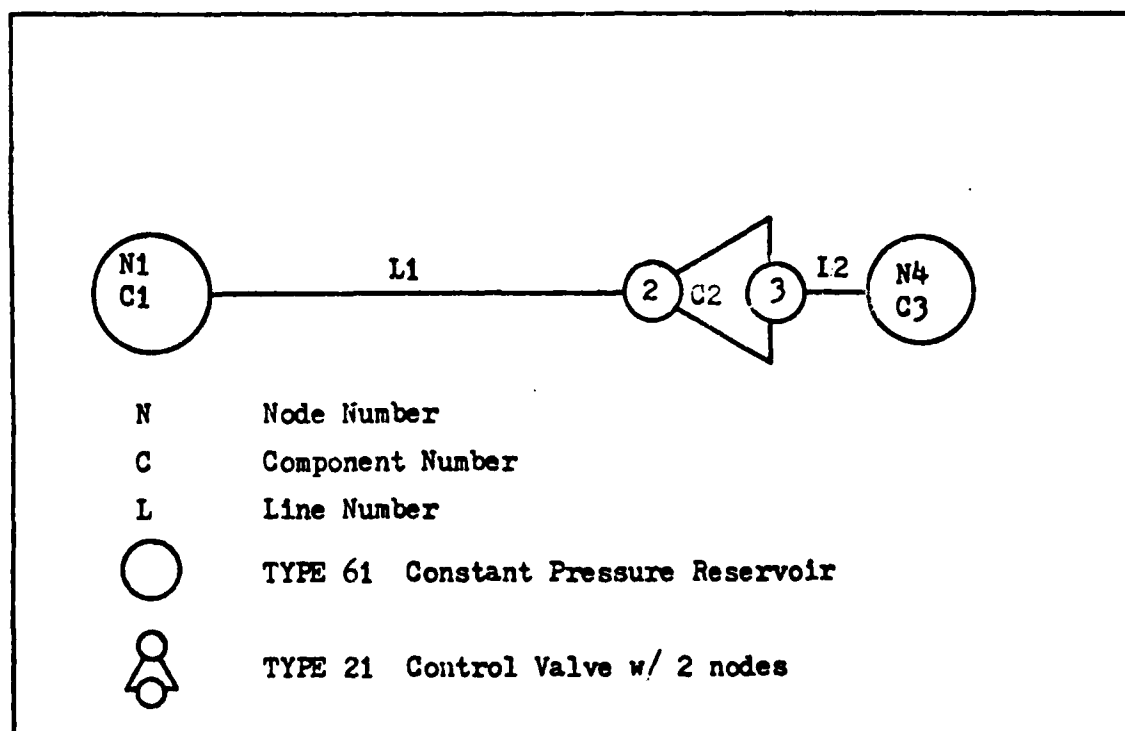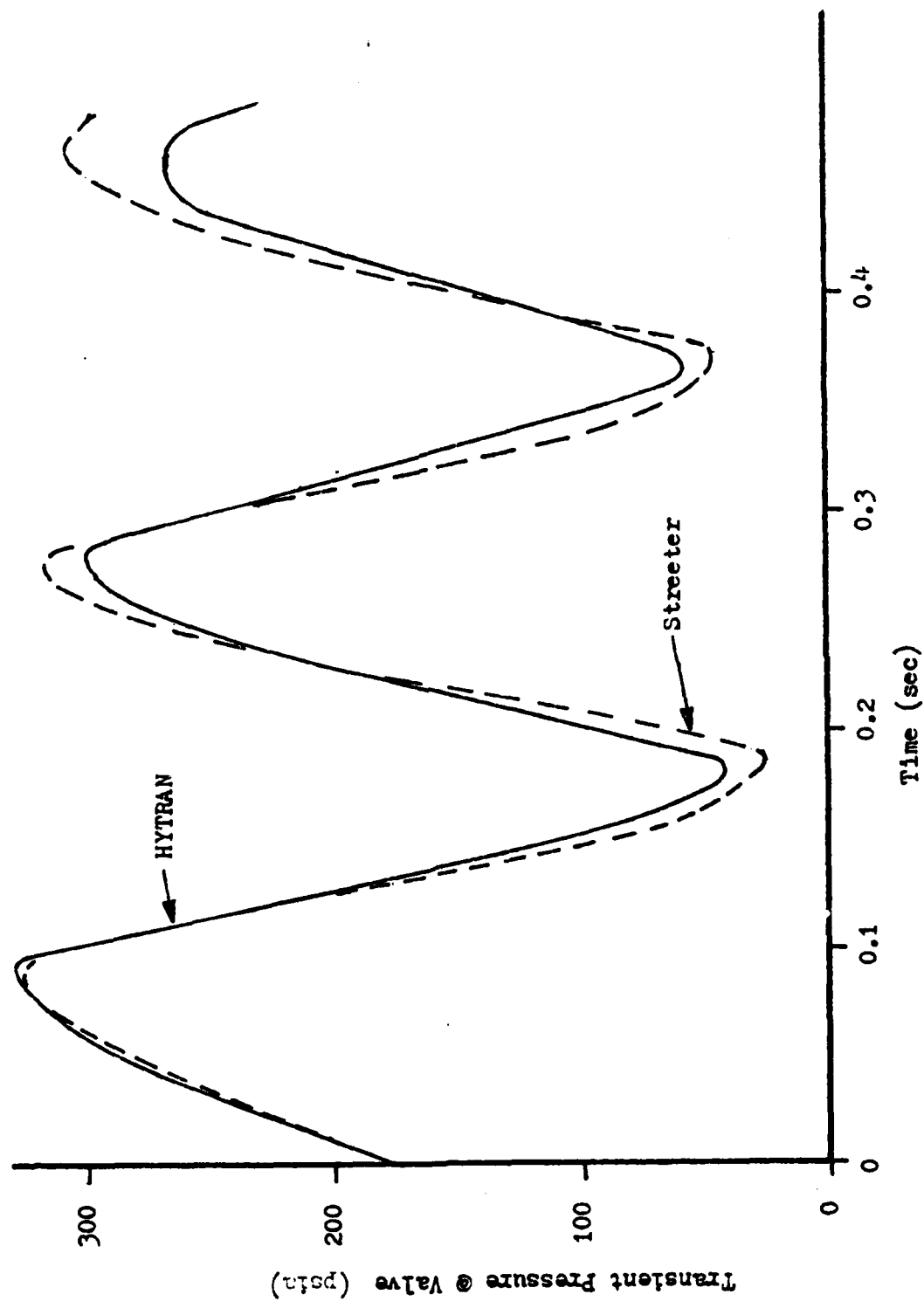|		
N	Node Number	
C	Component Number	
L	Line Number	
⬯	TYPE 61 Constant Pressure Reservoir	
⬯	TYPE 21 Control Valve w/ 2 nodes	

Fig 15. HYTRAN Diagram for Streeter's Experiment

Fig 16. Comparison of Transient Response Due to Valve Closure; HYTRAN versus Streeter

according to Eq (1) with K(t) from curve D of Chapter VI, Fig 12.
Closure time was 0.03 sec. An oscillograph trace of the experimental
response for the conditions of the simulation was obtained from the
test report (Ref 9:24).

Preliminary results exhibited reflected peaks not shown in the
experimental data that indicated the laboratory pumping system did
not reflect pressure waves precisely as a constant pressure reservoir.
As a result, the laboratory pumping system was modeled as a constant
pressure reservoir connected to a long line, the length of which
prevented the return of the reflected wave during the time interval
of interest (0.0 to 0.4 sec). The line from source to test section
(L1) was lengthened to accomplish this modification of the model.
The pressure of the constant pressure source was adjusted to provide
the desired steady state flow conditions.

Comparison of experimental and simulated transient response to
the valve closure is shown in Fig 17. The first peak in both cases
corresponds to the complete closure of the valve. Excellent agreement
is seen in comparison of the five percent settling times. The
settling time is the time required for the response to decrease to a
specified percentage of its final value. The initial and final
values are virtually the same for both.

Comparison of peak magnitudes and phasing are less favorable.
The computer simulation underpredicts the magnitude of the first peak
and overpredicts the subsequent peaks. There are twice as many peaks
in the experimental results as in the simulation; a result, perhaps,
of the accumulator model limitations.

Fig 17. Comparision of Experimental and Simulated Transient
Response at Nozzle to Valve Closure for the
Laboratory Test Model

Accumulator Volume and Precharge. Four accumulator volume
configurations with four different precharge settings per configuration
were investigated. All simulation conditions with the exception of
accumulator parameters were outlined in the previous section. Shown
in Figs 18-21 are the maximum transient pressures versus precharge
pressures for each volume configuration. Refer to Fig 3 for the
relative locations of the boom inlet and nozzle.

Fig 18. Effect of Accumulator Precharge on Maximum Transient Pressure for Accumulator Volume of 1000 cubic inches for the Laboratory Test Model

Fig 19. Effect of Accumulator Precharge on Maximum Transient
Pressure for Accumulator Volume of 660 cubic inches
for the Laboratory Test Model

41

Fig 20. Effect of Accumulator Precharge on Maximum Transient Pressure for Accumulator Volume of 500 cubic inches for the Laboratory Test Model

Fig 21. Effect of Accumulator Precharge on Maximum Transient Pressure for Accumulator Volume of 250 cubic inches for the Laboratory Test Model

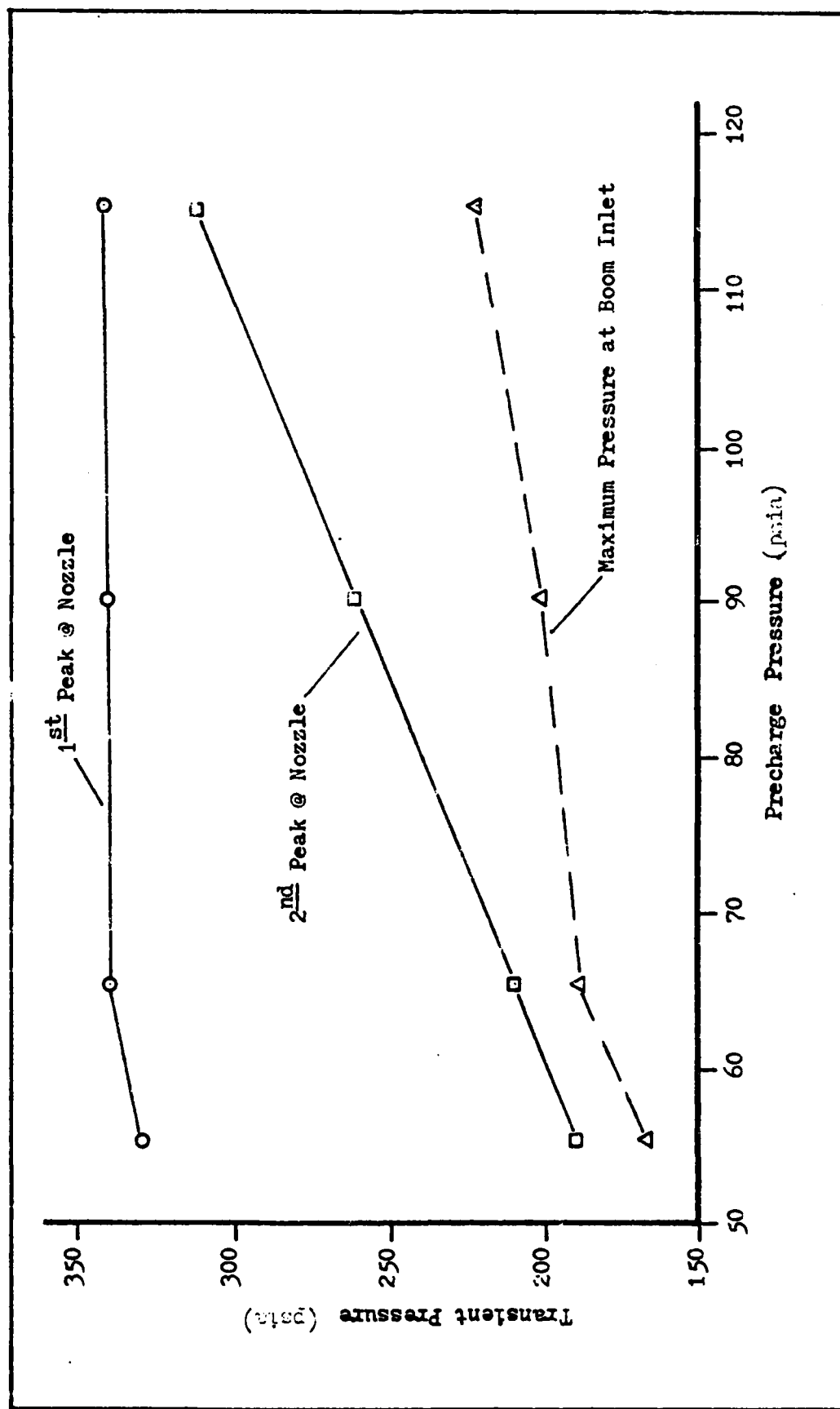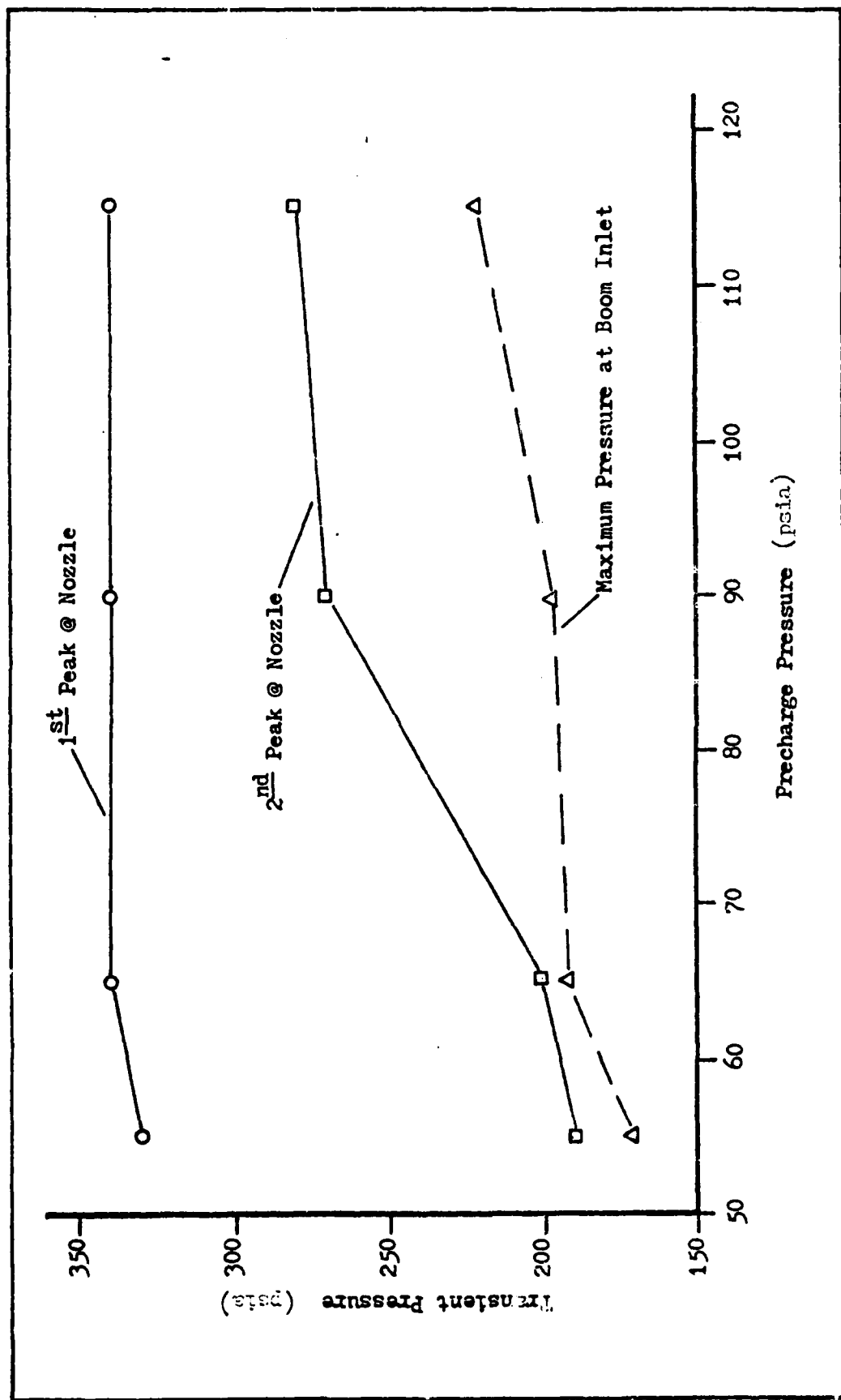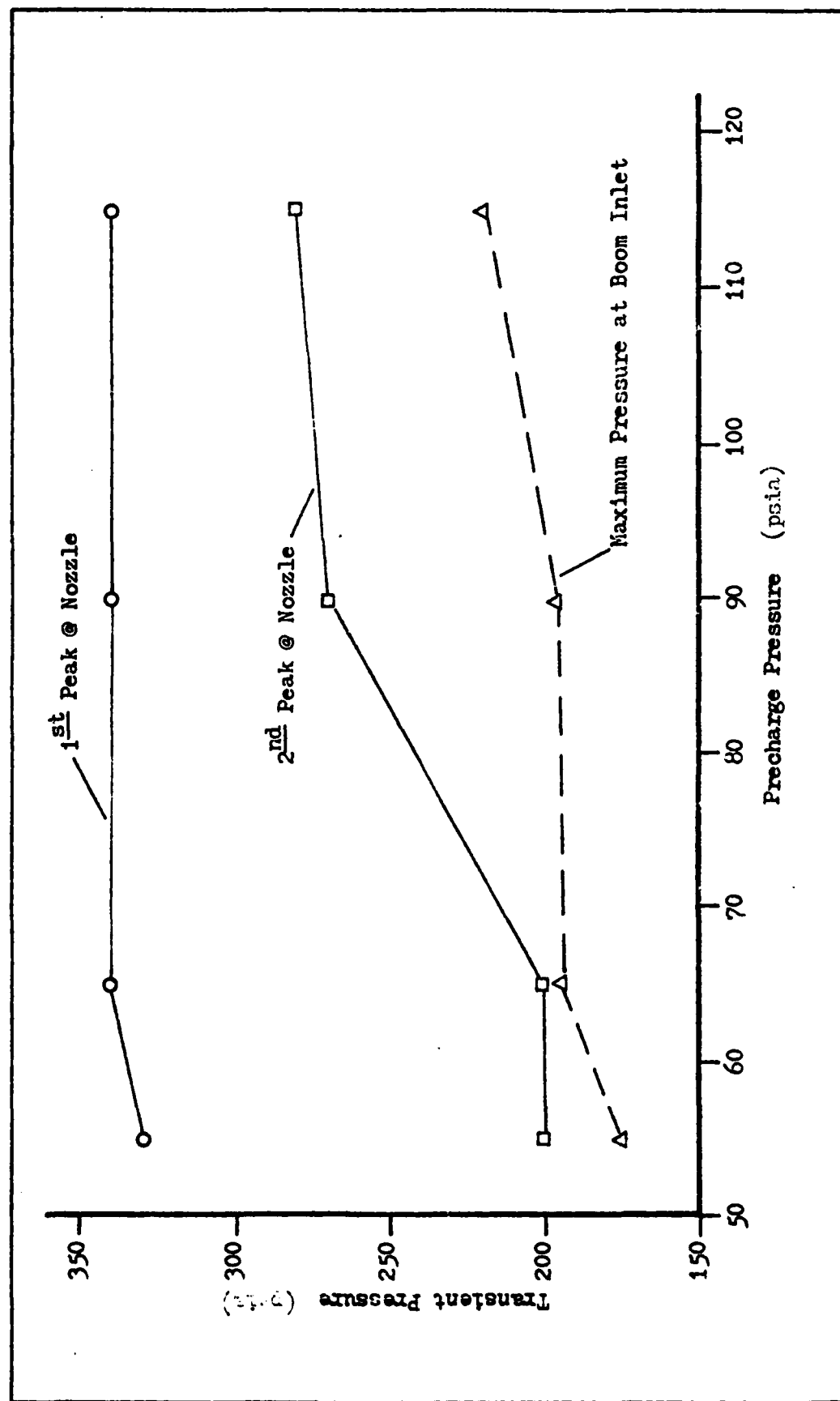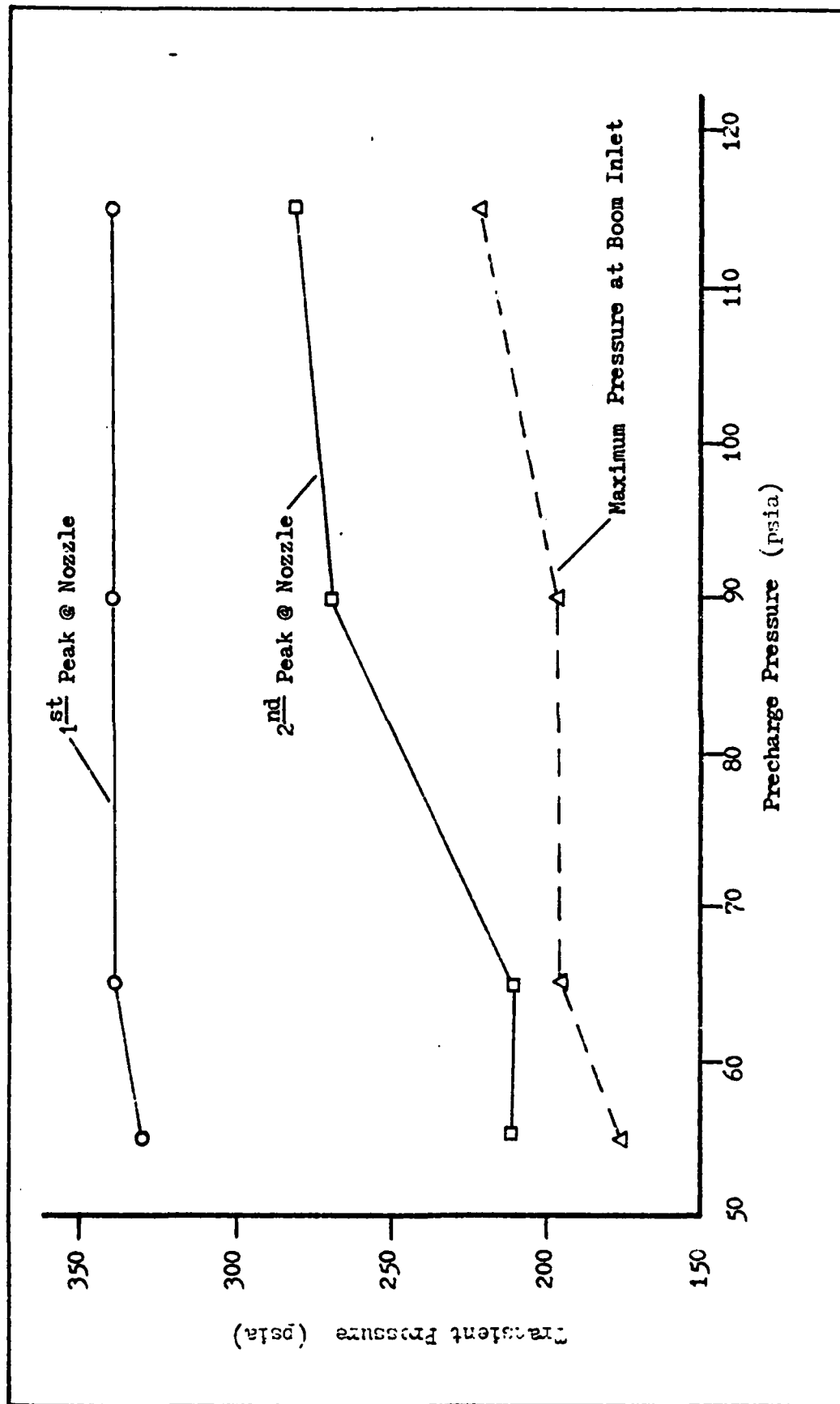Volume changes had a negligible effect on the maximum transient pressure at either the nozzle or boom inlet. A small change in the second peak pressures at low precharge as the volumes are decreased is due to the accumulators reaching their fluid capacity limits. The dominant influence was precharge pressure, increasing precharge pressure resulted in higher peak pressures at both nozzle and boom inlet. Note that the first peak is unaffected by changes in either volume or precharge. This is due to the accumulator time response lag. The initial impulse is not attenuated as readily as surges that build up over a longer period of time since a finite period of time is required for flow into the accumulators to begin.

Accumulator Entry Line Diameter. Simulations with accumulator entry line diameters from 1.25 to 2.75 in were run to observe the general effects of diameter variation. Also, since the actual accumulator entry line diameters for the Laboratory Test were not known, a verification of the choice of 1.75 in was desired. All simulation conditions except for entry line diameter were as outlined in the previous section. The basis for comparison was the maximum transient pressure, five percent settling time, and the number of peaks to settling time.

Changes in diameter did not affect the maximum pressure at the boom nozzle. As in the previous section, this is attributed to the accumulator response time. The maximum pressure at the boom inlet is affected because during the time required for the pressure wave to reach the boom inlet, flow into the accumulators has begun. The increase in pressure magnitude at the boom inlet for a decrease in the diameter is shown in Fig 22. This increase is expected due to the

Fig. 22. Effect of Variation of Accumulator Entry Line Diameter on Maximum Transient

Pressure at Boom Inlet for the Laboratory Test Model

additional resistance to flow in smaller pipes, thus negating some of the capability of the accumulator to function as an energy absorption component.

Settling time and number of peaks to settling time were favorably affected by decreasing the line diameter, Fig 23 and 24. Settling time was reduced by 20 to 50 percent for the range of diameters. The number of peaks from initiation to settling time was reduced 50 to 70 percent. In this case the increase in flow restriction to the accumulator resulted in increased damping and less pulsation added to the system due to the release of energy stored in the accumulators.

Two runs were made with longer than standard (14 in longer) accumulator entry lines. The results for the longer lines exhibited the same response trends as decreasing the diameter, see Fig 23.

Examination of settling times at the nozzle supports the choice of the 1.75 in entry line for the Laboratory Test simulation. The settling time of approximately 0.02 sec agrees with the measured response (Fig 17).

Closure Curve Study

Laboratory Test Model. Simulations were run using each of six closure curves, shown in Fig 25, to examine the effects of curve shape. Steady state conditions were as described in Chapter IV with an accumulator precharge of 90 psia. Valve closure was according to Eq (1) with $K(t)$ given by the closure curves. Time of closure was 0.03 sec.

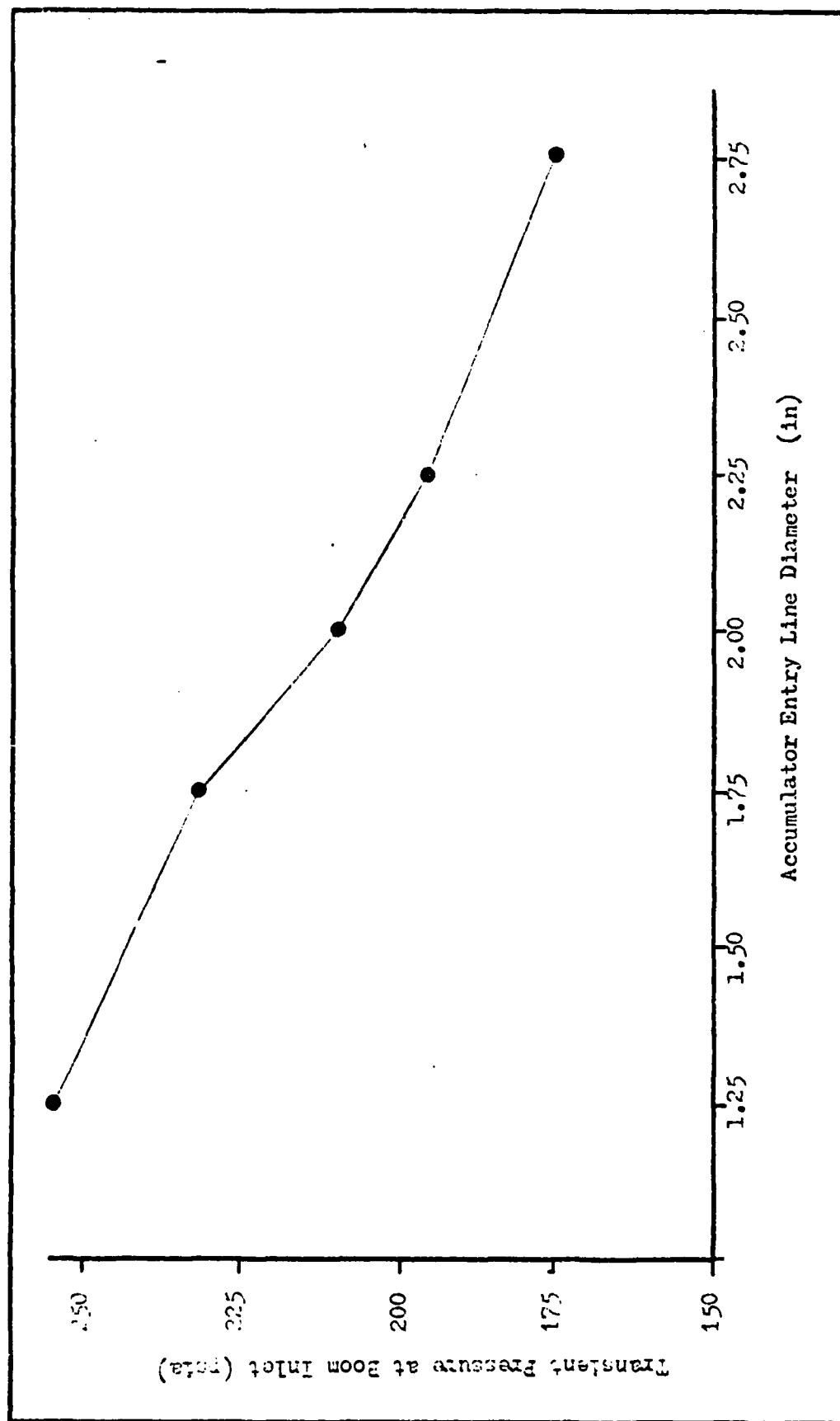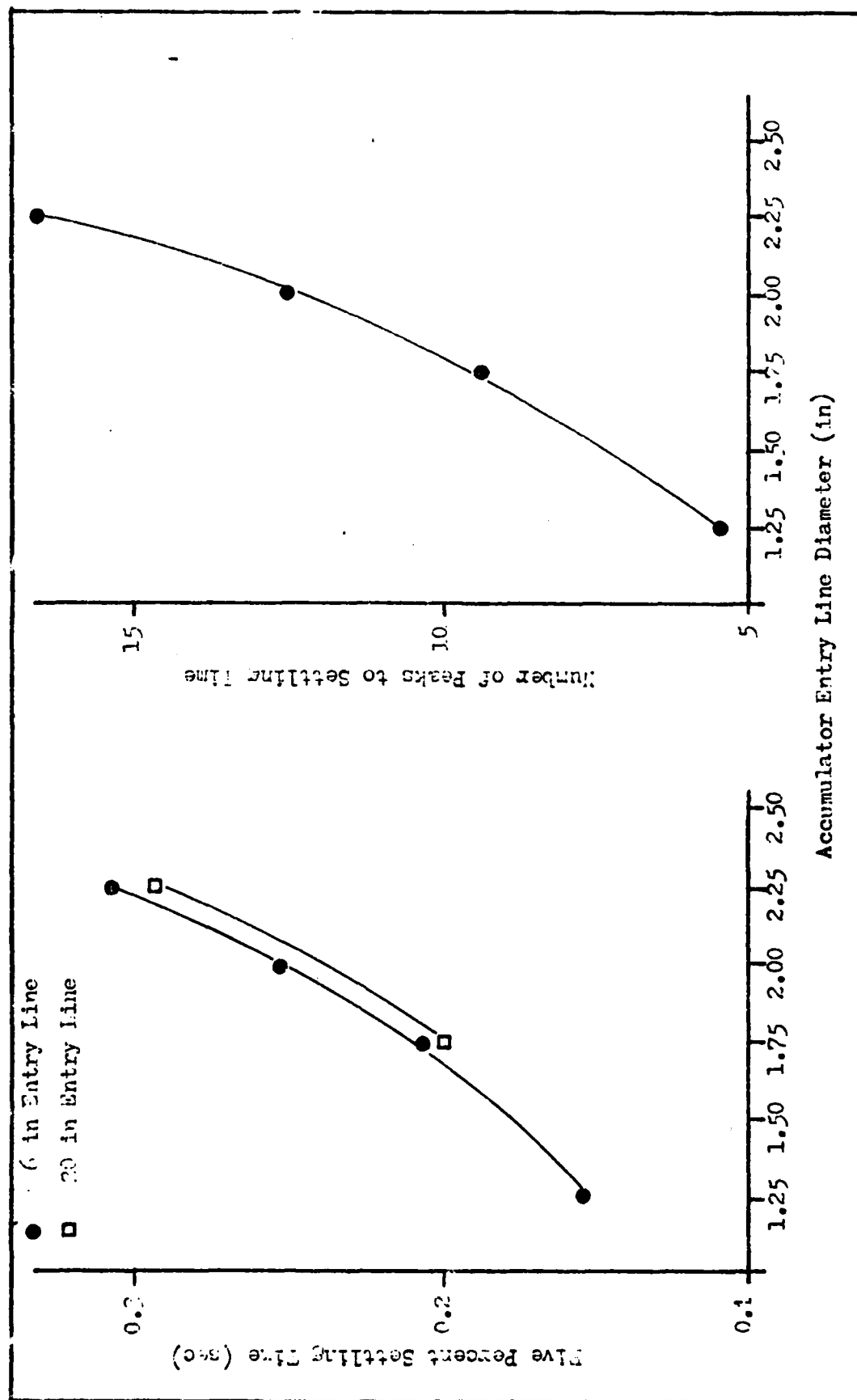Fig. 23. Effect of Variation of Accumulator Entry Line Diameter on Transient Response at Nozzle for the Laboratory Test Model
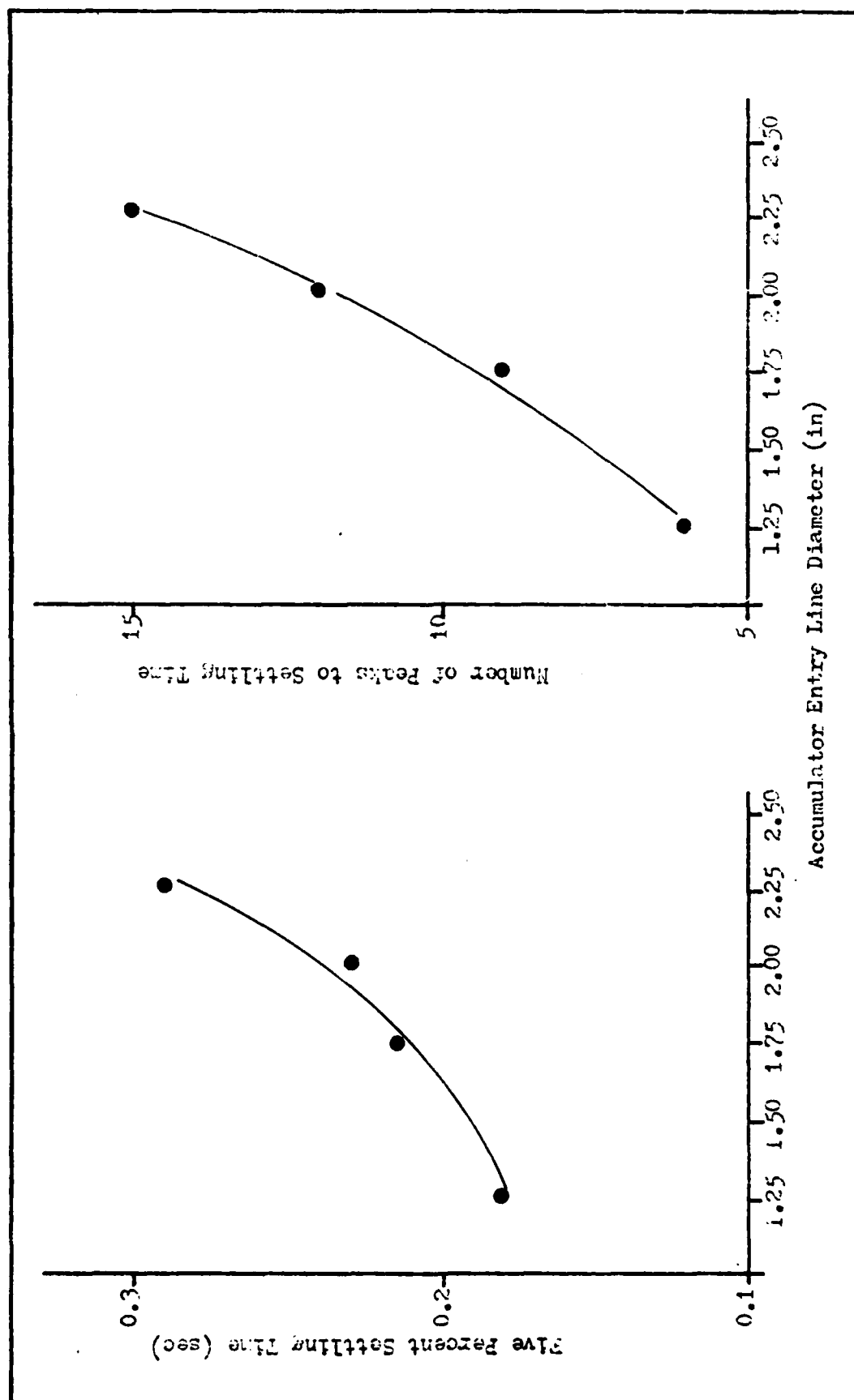
Fig. 24. Effect of Variation of Accumulator Entry Line Diameter on Transient Response at Boom
Inlet for the Laboratory Test Model
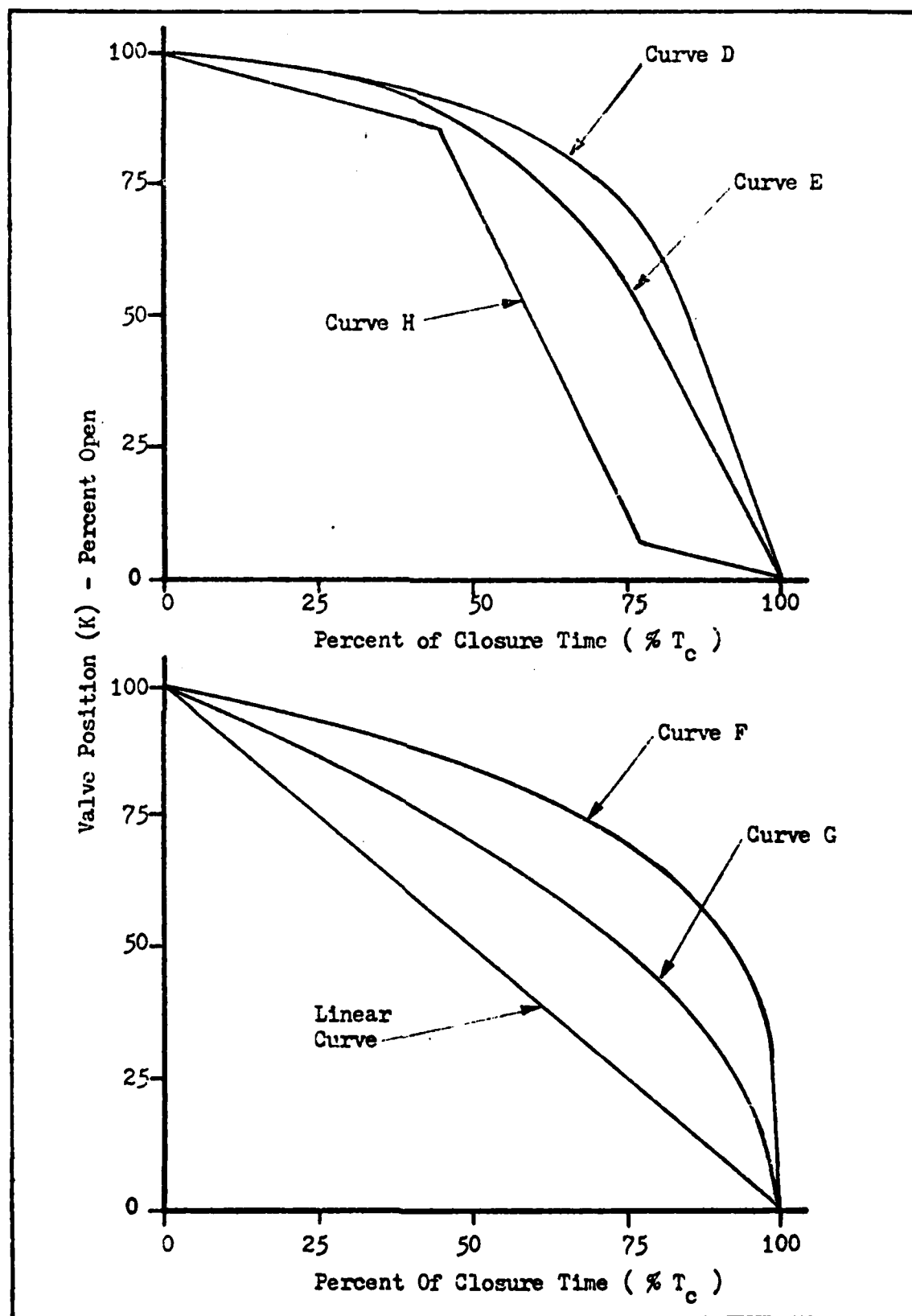
Fig 25. Closure Curves for Laboratory Test Model Closure
Curve Study

49

TABLE I

Effect of Curve Type on Transient Pressure and
Settling Time for the Laboratory Test Model

Maximum Transient Pressure (psia)

Curve	Nozzle	Boom Inlet	Settling Time (sec)
Linear	310	137	.243
D	340	210	.246
E	340	190	.232
F	340	206	.247
G	340	220	.247
H	260	122	.242

Results for the six curves are shown in Table I. Curves D, E, F,
and G, produced similar results, not unexpected since the general
curve shape is the same for all four (Refer to Fig 25). Maximum
transient pressure at the nozzle and boom inlet for those four curves
are the same except for curve E. Curve E has a less severe closure
which results in a slightly lower pressure at the boom inlet;
settling time is also shorter, again a reflection of the less severe
closure.

The linear closure resulted in a reduction of maximum transient
pressure at both the nozzle and boom inlet; settling time was
somewhat less than curves D, F, and G but greater than curve E. The
reduction in pressure was due to the constant rate of closure without
changes in slope.

Curve H yielded the lowest maximum transient pressure of the
group. Settling time was of the same order as the linear case. The

reduction in pressure peaks was due to the "snubbing" effect during the final stage of closure. This effect is examined further in the next section.

In Chapter VI curve D was selected as the representative curve shape for a quick disconnect; the results of this section indicate a similar response to curves D, E, F, and G; therefore, a general analytical relationship applicable to all and hence, a quick disconnect can be given as

$$K(t) = \left[1 - \frac{t}{T_c} \right]^m \qquad (8)$$

where $m < 1$

For the quick disconnect case, the linear and snubbed curves are not applicable because of the lower maximum pressures generated.

Valve Snubbing Effects. Valve snubbing was discussed in Chapter VI and is defined for this study as the reduction in the rate of valve area decrease during the final ten percent of valve area reduction. The effect of valve snubbing was investigated by running the Laboratory Test simulation with snubbed and unsnubbed curves. Time of closure and steady state conditions were the same as the previous runs. The valve closure was given by Eq (1) and $K(t)$ from the modified closure curve H as shown in Fig 26a. Four closures were evaluated; an unsnubbed curve, and three with snubbing of 3.7%, 7.5%, and 11%, respectively. The 7.5% snubbed curve is the basic curve H. The effect of the increased percentages of snubbing is shown in Fig 26b. Increasing the snubbing percentage decreases

(b) Effect of Valve Snubbing on Transient Pressure at Nozzle

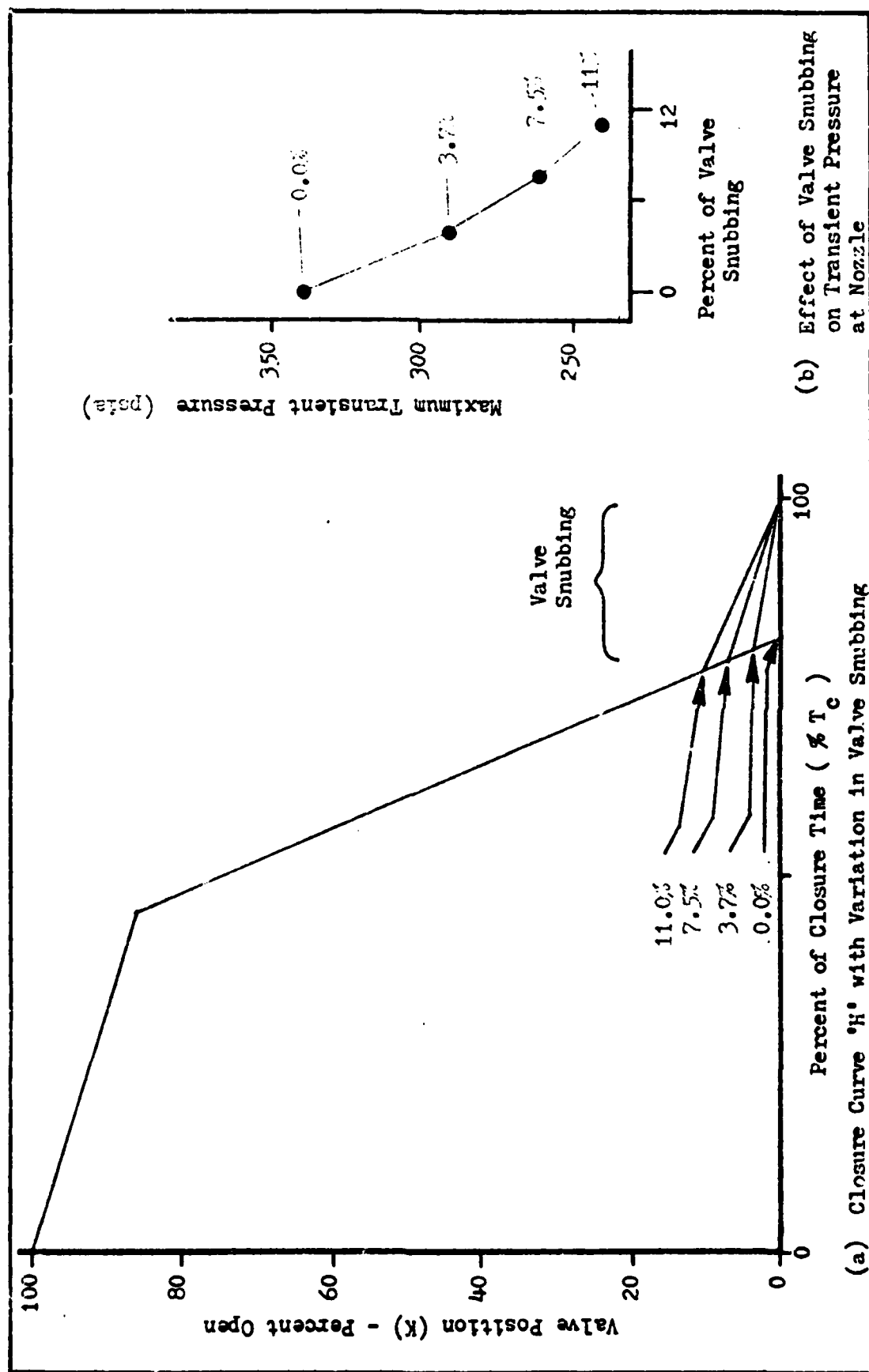(a) Closure Curve "H" with Variation in Valve Snubbing

Fig 26. Effect of Variation in Valve Snubbing on Transient Pressure

the maximum transient pressure.

KC-135 Model. The effect of closure curve shape and time of closure on the KC-135 system described in Chapter V was examined by varying the time of closure for several curves. The valve closure was given by Eq (1) with K(t) from closure curves A, B, C, E, F, G, H, and the linear curve. Time of closure was varied from 0.01 and 0.05 sec to encompass the minimum closure time discussed in Chapter VI and the minimum used by Parks (Ref 10:53). The surge boot precharge was 50 psig and all other conditions were as described in Chapter V.

The magnitude of the first peak at the nozzle was chosen as the basis for comparison of the results; the peak numbering is illustrated in Fig 27. The response of the system subsequent to the first peak was basically unaffected by changes in closure time curve shape. Normally the most important peak for design purposes is the first peak after valve closure, unless subsequent peaks are of greater magnitude. The latter case is possible in complex systems like the KC-135 where different concentrations of reflected pressure waves coalesce to form peaks greater than previous peaks. The transient response in Fig 27; closure curve A, T_c = 0.05 sec; is an example of such a case.

Shown in Fig 28 is the pressure of the first peak at the nozzle versus closure time for each curve.

For all curves there is an increasing pressure with decreasing closure time relationship. Curves E, F, and G are least affected by changes in closure time. These curves have closure rates that are high during the latter stages of closure thus most of the closure takes place over a short percentage of any closure time. The slope of the curve does not reverse, i.e., go from positive to negative or vice versa,
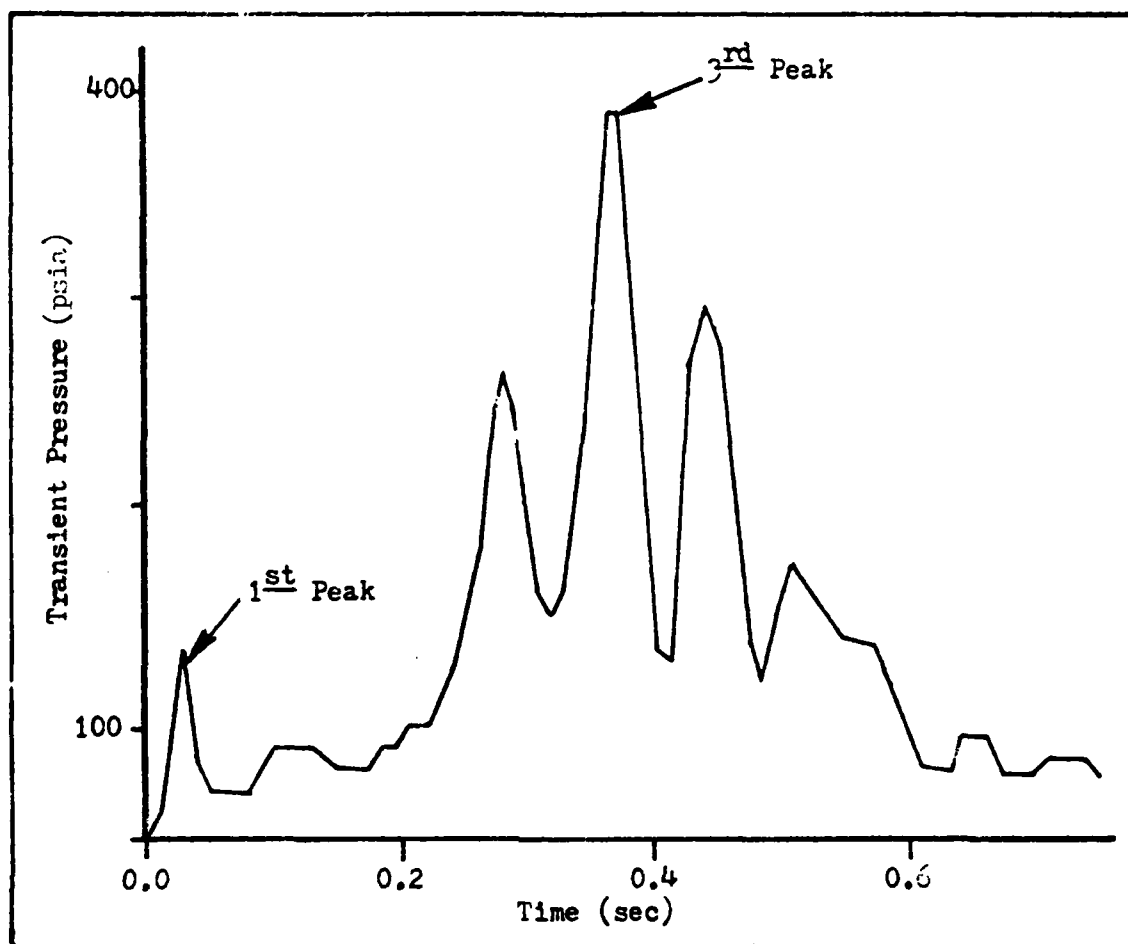
Fig 27. Numbering of Transient Pressure Peaks for a Typical Response to Valve Closure for the KC-135 Model using curve A and T_c = 0.05 sec.

over the closure interval.

Curves B, C, and H have similar responses to decreasing closure time. All of these curves appear to be very dependent on changes to closure time, especially below 0.03 seconds. The extreme effects of closure time variation is shown by the approximately 200% increase in pressure for a reduction in closure time from 0.03 to 0.01 sec.

The linear curve exhibits a relationship of pressure increase versus closure time that is similar to curves H, B, and C except that the increase is not quite so dramatic. This is a consequence of the constant slope with no snubbing.
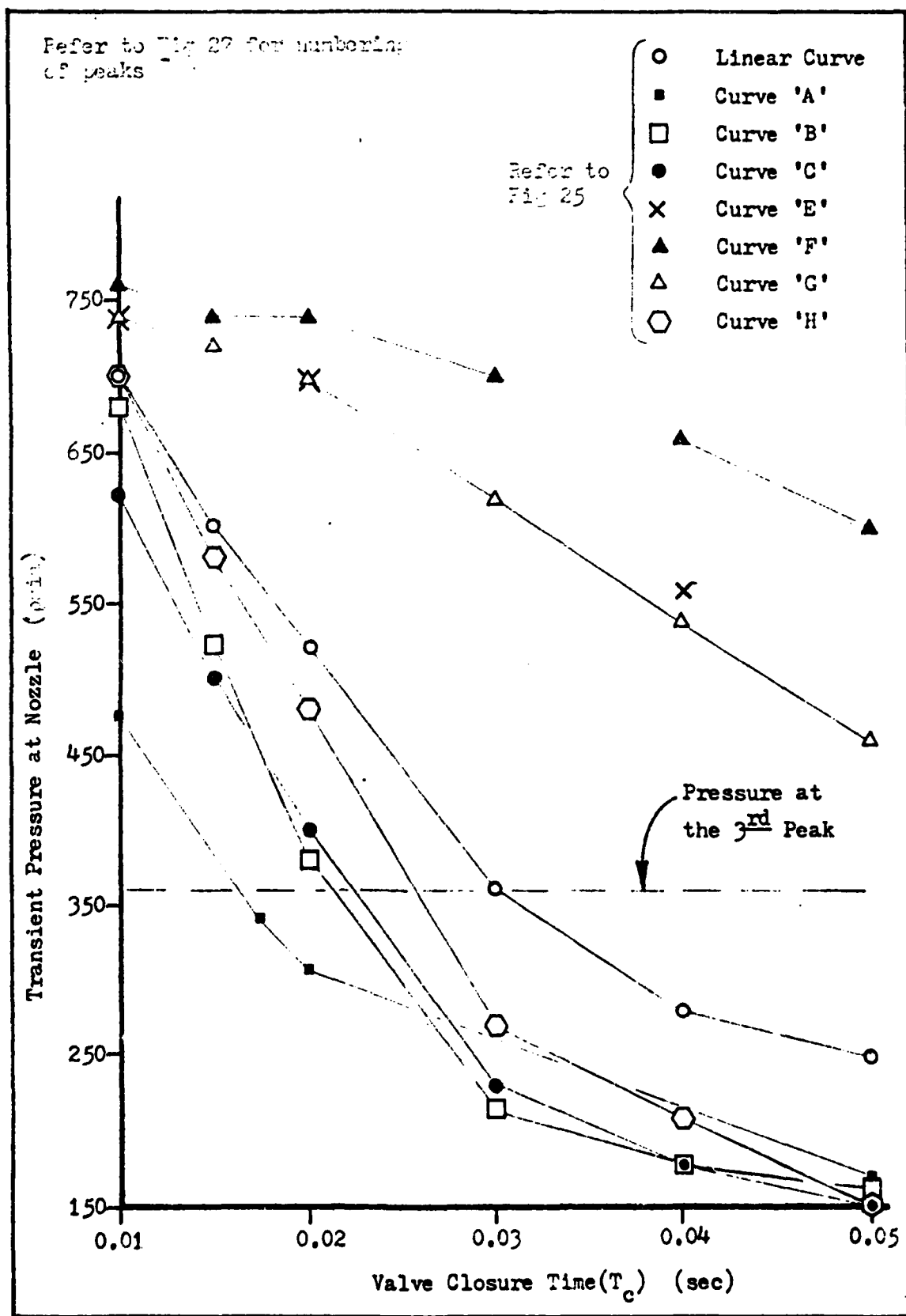
Fig 23. Effect of Closure Time Variation on 1ˢᵗ Peak
Transient Pressure for the KC-135 Model

Using curve A results in a modest change over the range of closure times. This is to be expected since the curve is heavily snubbed and has no reversal of slope. Note that neither curve A nor curves E, F, and G have slope reversals; the effect of changes in closure time is similar for all. The lower values of curve A are due to snubbing effects.

Overall, for the KC-135, the effect of reducing closure time is to shift the dominant pressure peak from the third peak to the first peak for all curves except E, F, and G. First peak pressure for all cases increases with reduction in closure time.

The consistency of the third peak value can be attributed to the system configuration, since for complex systems the compression wave initiated by the valve closure does not bring the flow to rest as it might in simple systems; therefore the time required for flow stoppage is characteristic of the system. As shown by Eq (3), a pressure peak will occur at the point of complete flow stoppage and dependent on the system, it is likely to maintain a consistent magnitude without regard to closure time. For the KC-135 model, complete flow stoppage occurs coincident with the timing of the third peak. This is illustrated in Fig 29 for a typical response upstream of the nozzle.

Parks (Ref 10:53-55) investigated pressure versus closure time for the interval 0.05 and 0.15 sec and found little change. For the closure used by Parks; curve A, $T_c = 0.05$ sec; the results previously discussed indicate that the third peak would be predominant and consistently the same magnitude. Therefore, the results Parks obtained are consistent with the results of this study.
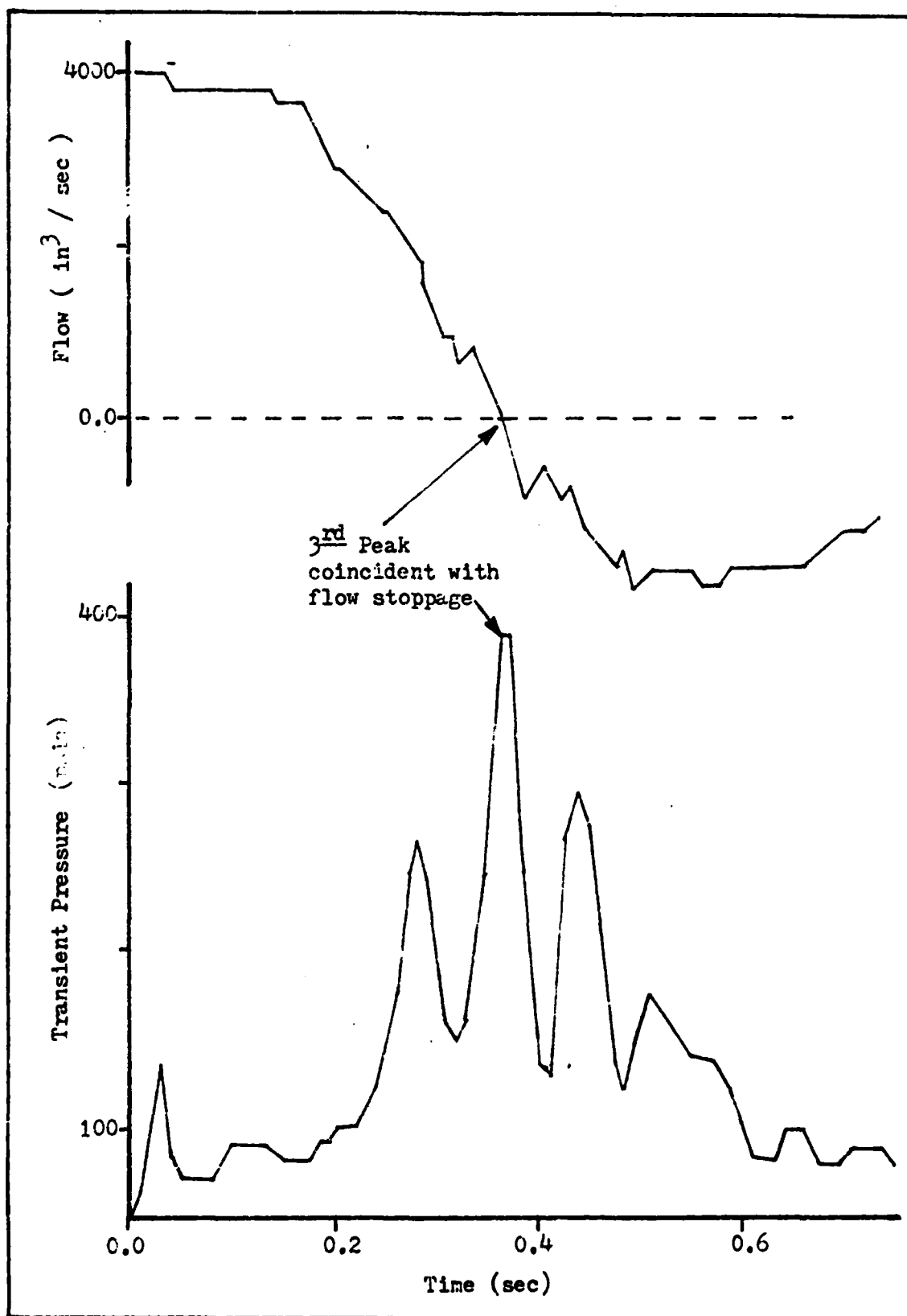
Fig 29. Typical Effect of Flow Stoppage on Transient Response
for the KC-135 Model using curve A and T_c = 0.05 sec

Variation of KC-135 Surge Boot Precharge Pressure

The effect of surge boot precharge was investigated by varying the precharge from 50 to 100 psig. A linear closure curve was used with closure times of 0.03 and 0.05 sec. All other conditions were as described in Section V.

Results, shown in Fig 30, indicate an increase in pressure for the first peak and a reduction in pressure for the third peak over the range of increasing precharge pressure. Nozzle pressure versus precharge pressure curve slopes for the first peak are similar for both closure times with a higher transient pressure for the 0.03 sec closure. The third peak has the same response for both closure times.

Parks' study (Ref 10:53) indicated a decreasing maximum transient pressure with increasing precharge pressure relationship. As discussed earlier, due to the slow closure (T_c = 0.05 sec) and extreme snubbing of the closure curve used by Parks, the third peak was predominant in his study. Therefore, the results obtained by Parks and the third peak results of this study are in agreement.

The differing effects on the first and third peaks result from the inability of the accumulator to respond quickly to short duration impulses. The third peak pressure builds at a slower rate as the flow decreases to zero. For the first peak, increasing the precharge pressure acts to harden the system, providing progressively less energy absorption for the impulse. Conversely, the slower building pressure of the third peak is attenuated with the increased precharge since more energy is required to compress the gas in the accumulators.

The effect of precharge for the KC-135 model is consistent with the results obtained for the Laboratory Test model. The Laboratory
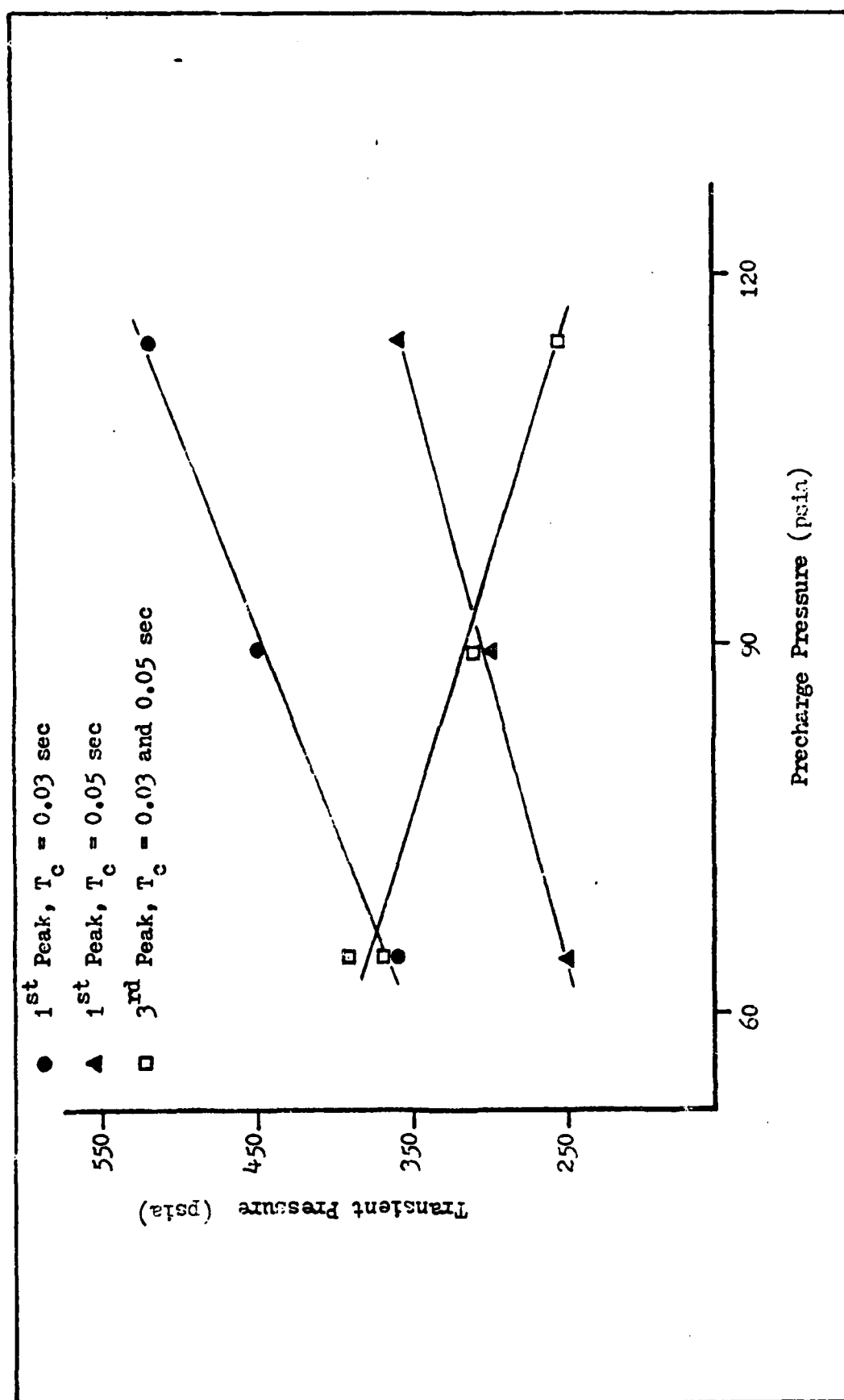
Fig 20. Effect of Variation in KC-135 Surge Boot Precharge on Transient Pressure at Nozzle

Test is a relatively simple system with the first peak predominant; the maximum pressure increased with precharge pressure increases.

VIII. Conclusions

Based on the research and simulations conducted and reported herein, it is concluded that:

1. The HYTRAN computer program can predict the transient response of simple systems with good results.

2. Simulation of the Laboratory Test resulted in a favorable agreement with experimental findings for the general transient response but underpredicted maximum transient pressure by approximately 15%.

3. For the Laboratory Test simulation:

a) A 75% decrease in accumulator volume with other variables held constant had a negligible effect on maximum transient pressure.

b) Increasing the accumulator precharge pressure with other variables held constant caused an increase in transient pressure.

c) Decreasing the diameter or increasing the length of the accumulator entry lines with all other variables held constant caused an increase in transient pressure and a decrease in the time required to settle to a steady pressure after valve closure.

4. The representative closure curve for quick disconnects must be derived from analysis of the combined nozzle/receptacle dynamics. The curve developed in this study gave good results when used in the Laboratory Test simulations and compared to the experimental results.

5. Increased percentages of valve snubbing decreases transient pressures; this is consistent with the findings of Kinzig (Ref 8).

4. For the KC-135:

a) The overall effect of decreasing nozzle valve closure time is to increase transient pressures; the dominant peak in the transient response is shifted from the third peak to the first peak; the third peak is essentially constant for all closure times.

b) Increasing the surge boot precharge pressure increased the first peak pressure and decreased the third peak pressure.

IX. Recommendations for Further Study

Additional verification of computer simulations with experimentally measured data is needed to gain confidence in the computer predictions. A scaled down system similar in configuration to the Laboratory Test could be used in the laboratory for parameter variation experiments.

A fuel systems oriented derivative of HYTRAN is available; this program, FUELTRAN, uses the basic HYTRAN program with additional subroutines added for fuel system component models (Ref 19). FUELTRAN was not used for this study because confidence could not be developed in the results obtained from it. FUELTRAN should be evaluated thoroughly to determine what, if any, usage limitations exist.

Bibliography

1. Wylie, Benjamin E. and Victor L. Streeter. _Fluid Transients_. New York: McGraw-Hill Book Company, 1978

2. Goodson, R.E. and Leonard, R.G. "A Survey of Modeling Techniques for Fluid Line Transients". _Journal of Basic Engineering_, Trans. ASME, Series D, Vol 94, No. 2, June 1952, PP. 474-482.

3. Streeter, Victor L. and Lai, Chintu. "Water-Hammer Analysis Including Fluid Friction", _Journal of the Hydraulics Division_, Proc. ASCE, Vol. 88, No. HY3, May 1962, PP. 79-112.

4. McDonnell Aircraft Company, McDonnell Douglas Corporation, St. Louis _Aircraft Hydraulic Systems Dynamic Analysis_. Air Force Aero Propulsion Laboratory Technical Report, AFAPL-TR-76-43, Vol II, February 1977.

5. McDonnell Aircraft Company, McDonnell Douglas Corporation, St.Louis _Advanced Fluid Systems Simulation_. Air Force Wright Aeronautical Laboratories Technical Report, AFWAL-TR-80-2039, April 1980.

6. McDonnell Aircraft Company, McDonnell Douglas Corporation, St.Louis _Aircraft Hydraulic Systems Dynamic Analysis_. Air Force Aero Propulsion Laboratory Technical Report, AFAPL-TR-77-63, October 1977.

7. Parks, S.E. and Franke, M.E. _Transient Flow Analysis of an Aircraft Refueling System_. American Institute of Aeronautics and Astronautics Paper No. 81-164-1, 1981.

8. Kinzig, William et al. _KC-10 Aerial Refueling Surge Pressure Analysis_. Aeronautical Systems Division Technical Memorandum, ENFEM-TM-80-10, December 1980.

9. Douglas Aircraft Company, McDonnell Douglas Corporation, St.Louis. _Advanced Aerial Refueling Boom/Advanced Aerial Refueling Nozzle Boom/Nozzle Disconnect Surge_. MDC Report J7717, September 1977.

10. Parks, Scott E. _Dynamic Characteristics of the KC-135 Refueling System_. MS Thesis. Wright-Patterson AFB, Ohio: Air Force Institute of Technology, December 1980.

11. 4950th Test Wing Report, GTR-80-13, _Improved Aerial Refueling Pump System (IARPS) KC-135 Ground Test_. Wright-Patterson AFB, Ohio: 4950th Test Wing, August 1980.

12. United States Air Force T.O. 1-C-135(K)A-2-6, U.S.A.F. Series
KC-135 Air Refueling (A/R) System, Oklahoma Air Logistics Center,
Tinker AFB, OK, February 1966.

13. Patterson, William B. et al. User Guide for Aircraft Hydraulic
Systems Dynamic Analysis Volume I Transient Analysis (HYTRAN)
Computer Program User Manual. Flight Test Technology Branch
Office Memo, Edwards AFB, CA: 6510 Test Wing, January 1981.

14. McDonnell Aircraft Company, McDonnell Douglas Corporation, St.Louis
Aircraft Hydraulic Systems Dynamic Analysis. Air Force Aero
Propulsion Laboratory Technical Report, AFAPL-TR-76-43, Vol. I,
February 1977.

15. McDonnell Aircraft Company, McDonnell Douglas Corporation,
St. Louis. Aircraft Hydraulic Systems Dynamic Analysis-
Component Data Handbook. Air Force Wright Aeronautical
Laboratories Technical Report, AFWAL-TR-80-2040, April 1980.

16. McDonnell Aircraft Company, McDonnell Douglas Corporation,
St. Louis. KC-10A Aerial Refueling System Interface Control
Document Spec Type B1. Specification No. ZA015800, November 1980

17. Kinzig, William. Data Input for KC-10 HYTRAN Model used in Ref 3.
Mechanical Branch, Flight Equipment, Directorate of Flight Systems
Engineering, Wright-Patterson AFB, Ohio. March 1982.

18. Baumeister, Theodore et al. Marks Standard Handbook for
Mechanical Engineers. New York; McGraw-Hill Book Company, 1978

19. Kinzig, William. Fuel Transient Analysis (FUELTRAN) Computer
Program Technical Description Manual. Aeronautical Systems
Division Technical Memorandum, ENFEM-TM-81-03, Vols I and II,
March 1981

APPENDIX A

Input Data for the Laboratory Test Model

TABLE II

Input Data for the Laboratory Test Model

TABLE II, continued

NUMBER OF NODES = 13   NUMBER OF LEGS = 12   NUMBER OF CONSTANT PRESSURE NODES = 0

LEG CONNECTION INPUT DATA

LEG NO	UPST NODE NO	DNST NODE NO	NO OF ELEMENTS	FLOW GUESS	UPST PRESS	DNST PRESS
1			3	2013.00000	0.00000	0.00000
2			3	2013.00000	0.00000	0.00000
3			1	2014.00000	0.00000	0.00000
4			1	2014.00000	0.00000	0.00000
5			2	2013.00000	0.00000	0.00000
6			2	2013.00000	0.00000	0.00000
7			2	2013.00000	0.00000	0.00000
8			3	0.00000	0.00000	0.00000
9				0.00000	0.00000	0.00000
10				0.00000	0.00000	0.00000
11				0.00000	0.00000	0.00000

APPENDIX B

Input Data for the KC-135 Model

TABLE III

Input Data for the KC-135 Model

ITEM NO.	LENGTH	INTERNAL DIA	WALL THICKNESS	MODULUS OF ELASTICITY	DELX	CHARACTERISTIC IMPEDANCE	VELOCITY OF SOUND
1	1.0000	3.4560	.0720	.100E+06	1.0000	.2240	2000.0000
2	1.0000	3.4560	.0720	.100E+06	1.0000	.2240	2000.0000
3	1.0000	3.4560	.0720	.100E+06	1.0000	.2240	2000.0000
4	1.0000	3.4560	.0720	.100E+06	1.0000	.2240	2000.0000
5	10.0000	3.4560	.0720	.100E+04	10.0000	.2240	2000.0000
6	10.0000	3.4560	.0720	.100E+05	18.6667	.2240	33976.4744
7	3.0000	1.4400	.0300	.100E+04	13.0000	1.6433	34757.4500
8	3.0000	3.4560	.0720	.100E+04	19.0000	.2240	33976.4744
9	17.0000	3.4560	.0720	.100E+04	17.1667	.2240	33976.4744
10	18.0000	3.4560	.0720	.100E+04	18.0000	.2240	33976.4744
11	24.0000	3.4560	.0720	.100E+04	24.0000	.2240	33976.4744
12	20.0000	3.4560	.0720	.100E+04	17.3333	.2240	33976.4744
13	42.0000	3.8550	.0720	.100E+08	21.0000	.2240	33976.4744
14	4.0000	3.4560	.0720	.100E+04	21.0000	.2240	33976.4744
15	12.0000	1.4400	.0300	.100E+04	13.0000	1.6433	34757.6500
16	170.0000	3.4560	.0720	.100E+04	17.0000	.2240	33976.4744
17	104.0000	3.4560	.0720	.103E+04	17.3333	.2240	33976.4744
18	44.0000	3.8550	.0720	.100E+03	22.0000	.2240	33976.4744
19	35.0000	2.9840	.0590	.100E+08	17.5000	.4053	34503.4763
20	56.0000	3.4560	.0720	.100E+08	18.6667	.2240	33976.4744
21	56.0000	.7400	.0300	.100E+08	24.0000	4.1575	37470.0067
22	240.0000	6.0000	.1250	.100E+04	19.1539	.2234	37304.0764
23	3.0000	4.4260	.1020	.103E+04	20.7500	.1774	35404.1730
24	17.7000	4.4240	.1020	.100E+04	17.0000	.1774	35000.0000
25	46.0000	4.4240	.1020	.100E+03	26.0000	.1774	35000.1200

A... TBL,continued

27	1.5000	1.5000	.0720	.100E+01	1.0000	.2735	2235.0000
28	17.7	4.8270	.1570	.100E+01	17.7030	.1774	35400.0000
29	17.7000	4.8270	.1620	.100E+08	17.7030	.1774	35400.000
30	17.7000	4.8270	.1620	.100E+08	17.7030	.1774	35400.000
31	17.7000	4.8270	.1320	.100E+08	17.7030	.1774	35400.000
32	17.7000	4.8240	.1320	.100E+08	17.7030	.1774	35400.000
33	17.7000	4.8260	.1020	.100E+08	17.7030	.1774	35400.000
34	17.7000	4.8260	.1020	.100E+08	17.7030	.1774	35400.000
35	17.7000	4.8260	.1320	.100E+08	17.7030	.1774	35400.000
36	17.7010	4.8260	.1320	.100E+08	17.7030	.1774	35400.000
37	1.0000	1.9700	.0400	.105E+03	1.0000	.8735	2235.0000
38	1.0010	1.9700	.0400	.105E+03	1.0000	.8735	2000.0000
39	1.0000	1.9700	.0400	.100E+04	1.0000	.8735	2000.0000
40	1.0000	1.9700	.0400	.100E+04	1.0000	.8735	2000.0000
41	1.0000	1.9700	.0400	.103E+03	1.0000	.8735	2000.0000
42	1.0000	1.9700	.0400	.100E+04	1.0000	.8735	2000.0000
43	1.0000	1.9700	.0400	.100E+04	1.0000	.8735	2000.0000
44	1.0000	1.9700	.0400	.100E+04	1.0000	.8735	2000.0000
45	1.0000	1.9700	.0400	.100E+04	1.0000	.8735	2000.0001
46	1.0000	1.9700	.0400	.100E+04	1.0000	.8735	2000.0000
47	1.0000	1.9700	.0400	.100E+04	1.0000	.8735	2000.0000
48	1.0000	1.9700	.0400	.100E+04	1.0000	.8735	2001.0000
49	1.0000	1.4400	.0300	.100E+04	1.0000	1.6433	2001.0000
50	1.0000	1.4400	.0300	.100E+04	1.2000	1.6433	2000.0000

COMPT, 1 INTEGER DATA 1 61 1 1 3 0 0 0 0

REAL DATA CARD 1 .54706 = 0. 0. -1 0 0. 0. 0. 0.

TABLE III, continued

TABLE III, continued

TABLE III. continued

NUMBER OF NODES = 40   NUMBER OF LEGS = 39   NUMBER OF CONSTANT PRESSURE NODES = 0

LEG CONNECTION INPUT DATA

LEG NO	UPST NODE NO	DWST NODE NO	NO OF ELEMENTS	FLOW GUESS	UPST PRESS	DWST PRESS
1	1	4	5	1500.00000	0.00000	0.00000
2	2	5	5	1500.00000	0.00000	0.00000
3	3	6	5	1500.00000	0.00000	0.00000
4	6	7	5	500.00000	0.00000	0.00000
5	7	10	5	3000.00000	0.00000	0.00000
6	8	11	5	4500.00000	0.00000	0.00000
7	9	12	5	4500.00000	0.00000	0.00000
10	16	11	5	4500.00000	0.00000	0.00000
11	11	12	5	4500.00000	0.00000	0.00000

TABLE III. continued

Thomas J. Carter III was born 3 August 1947 in Louisville, Kentucky. He graduated from high school in Jackson, Tennessee in 1965 and entered the USAF in April 1966. He was assigned to the 3550th Field Maintenance Squadron at Moody AFB, Georgia until June 1967; from June 1967 until March 1969 he served with the 20th Special Operations Squadron in Southeast Asia. During the period March 1969 to September 1974 his assignments were to the 6510th Field Maintenance and Civil Engineering Squadrons, Edwards AFB, California; the 3550th Air Base Group (Civil Engineering), Moody AFB, Georgia; and the 5010th Civil Engineering Squadron, Eielson AFB, Alaska. He entered the Airman Education and Commissioning Program in October 1974 at Auburn University from which he received the degree of Bachelor of Mechanical Engineering in August 1977. He received his commission through OTS in December 1977. He then served as a flight test engineer, 6520th Test Group, Edwards AFB, California, until entering the School of Engineering, Air Force Institute of Technology, in June 1981.

Permanent Address: 506 N. Royal Street
Jackson, Tennessee
38301

REPORT DOCUMENTATION PAGE		READ INSTRUCTIONS BEFORE COMPLETING FORM
1. REPORT NUMBER AFIT/GAE/AA/82D-4	**2. GOVT ACCESSION NO.** AD-A124770	**3. RECIPIENT'S CATALOG NUMBER**
4. TITLE *(and Subtitle)* DYNAMIC CHARACTERISTICS OF AERIAL REFUELING SYSTEMS		**5. TYPE OF REPORT & PERIOD COVERED** MS Thesis
		6. PERFORMING ORG. REPORT NUMBER
7. AUTHOR(s) Thomas J. Carter III Captain		**8. CONTRACT OR GRANT NUMBER(s)**
9. PERFORMING ORGANIZATION NAME AND ADDRESS Air Force Institute of Technology (AFIT-EN) Wright-Patterson AFB, Ohio 45433		**10. PROGRAM ELEMENT, PROJECT, TASK AREA & WORK UNIT NUMBERS**
11. CONTROLLING OFFICE NAME AND ADDRESS 4950th Test Wing/FFDF Capt. Scott E. Parks Wright-Patterson AFB, Ohio 45433		**12. REPORT DATE** December,1982
		13. NUMBER OF PAGES 89
14. MONITORING AGENCY NAME & ADDRESS*(if different from Controlling Office)*		**15. SECURITY CLASS.** *(of this report)* Unclassified
		15a. DECLASSIFICATION/DOWNGRADING SCHEDULE

16. DISTRIBUTION STATEMENT *(of this Report)*

Approved for public release; distribution unlimited

17. DISTRIBUTION STATEMENT *(of the abstract entered in Block 20, if different from Report)*

18. SUPPLEMENTARY NOTES

Approved for public release; IAW AFR 190-17

Approved for public release: IAW AFR 190-17.

LYNN E. WOLAVER
Dean for Research and Professional Development
Air Force Institute of Technology (AIC)
Wright-Patterson AFB OH 45433

6 JAN 1983

19. KEY WORDS *(Continue on reverse side if necessary and identify by block number)*

Refueling Systems
Transient Flow Analysis
KC-135, Refueling System Computer Model

20. ABSTRACT *(Continue on reverse side if necessary and identify by block number)*

Two aircraft refueling system configurations were simulated using HYTRAN, an existing transient flow analysis computer program. Transient pressure response subsequent to downstream valve closure was investigated for the KC-135 and a laboratory test rig and compared to available experimental data and previous research. Parametric studies were performed of system variables: valve closure time, valve area versus time (closure curves), and variations in surge attenuation components

DD FORM 1 JAN 73 **1473** EDITION OF 1 NOV 65 IS OBSOLETE

(surge boot, accumulators). A typical closure curve for quick disconnects was approximated and verified. The simulation results compared favorably with experimental data and previous work. Transient pressure was found to be sensitive to accumulator or surge boot precharge pressure while changes in accumulator volume had little effect. Variations in accumulator entry line diameter or length affected transient pressure and settling time. Increased valve snubbing reduced maximum transient pressures.

END

FILMED

3-83

DTIC